Pressure Drop, Liquid Holdup, and Flow Regime Transition in Trickle Flow

R. A. Holub, M. P. Dudukovic, and P. A. Ramachandran
Chemical Reaction Engineering Lab., Washington University, St. Louis, MO 63130

A phenomenological, pore-scale, hydrodynamic model is developed for representation of the uniform, cocurrent, two-phase flow in the low interaction regime in trickle bed reactors. Comparison of model predictions with numerous pressure drop and liquid holdup data reveals that phase interaction terms are negligible which results in a simplified model with no adjustable parameters. This model yields improved pressure drop and liquid holdup estimates for the low interaction regime. In addition, a criterion for the prediction of the trickle to pulsing flow regime transition is developed based on Kapitza's (1945) work on laminar film stability. This criterion compares favorably to data and to some other existing models for prediction of the trickle to pulsing flow regime transition.

Introduction

In trickle bed reactors, gas and liquid flow cocurrently downward over a packed bed of catalyst particles. This reactor configuration assures flexibility of operation and high throughputs and is used extensively in hydrotreating processes of petroleum refining and in many gas-liquid-solid catalytic reactions of the chemical industry (Ramachandran and Chaudhari, 1983; Dudukovic and Mills, 1986; Ramachandran et al., 1987). Several flow regimes exist in trickle beds and are given descriptive names such as trickle, pulsing, spray, and dispersed bubble. The hydrodynamic and transport properties are dependent on these flow patterns. Therefore, it is important to predict pressure drop, liquid holdup, transport coefficients, and identify *a priori* the prevailing flow regime as a function of the operating variables and physical properties of the system of interest. Of particular interest is the widely used trickle flow, or low interaction regime, typically encountered at low liquid superficial velocities (up to 0.5 cm/s) and low gas superficial velocities (up to 300 cm/s) in which the gas is the continuous phase while liquid dribbles downward over the packing in the form of rivulets and films.

Numerous past studies of cocurrent downward gas-liquid flow in packed beds concentrated on either developing pressure drop and/or liquid holdup correlations or on establishing flow regime boundaries. We summarize here briefly the studies most pertinent to this work.

Hydrodynamics of two-phase cocurrent downflow: pressure drop and liquid holdup

The existing hydrodynamic models are of two classes. The first class uses an empirical approach based on dimensional analysis to produce explicit correlations for pressure drop and holdup (Larkins et al., 1961; Turpin and Huntington, 1967; Sato et al., 1973a; Midoux et al., 1976; Clements and Schmidt, 1980; Sai and Varma, 1987; Ellman et al., 1988, 1990). The second class involves modification of the single-phase flow Ergun equation to account for the existence of a second flowing phase. While the Ergun equation for single-phase flow has a fundamental basis, as it arises from a momentum balance in an assumed pore geometry, only heuristic arguments have been used to modify it for two-phase flow. The models presented by Sweeney (1967), Specchia and Baldi (1977), and Sáez and Carbonell (1985) fall in this category and are pertinent to this study.

The Ergun (1952) equation is widely used to predict single-phase flow pressure drop in packed beds. Ergun proposed the use of an equivalent spherical particle diameter and suggested universal values, independent of packing type, of the leading constants for the two terms in the equation. In a comprehensive comparison of the single-phase pressure drop predictions by the Ergun equation and data, MacDonald et al. (1979) concluded that while the functional form of the equation represents data well, very large errors (up to two orders of magnitude) are caused by the use of universal Ergun constants. They suggested that the constants be determined on each packing of interest.

R. A. Holub is currently with Ethyl Corporation, P.O. Box 341, Baton Rouge, LA 70821.

Several approaches have been used in applying the Ergun equation to two-phase flow in packed beds. Sweeney (1967) assumed the single-phase flow Ergun equation for each phase if the void volume available for flow of a phase is reduced to the volume occupied by the phase. Since the liquid was assumed to be contacting the particles, the particle size seen by the gas was increased and the average gas velocity was taken relative to the average liquid velocity. He compared the model to pressure drop data and found the best agreement when he changed his assumptions so that the solid particle size remained unchanged and the liquid was considered a solid boundary relative to the gas. No comparison was made to liquid holdup data even though total liquid holdup can be predicted by the model. Sweeney also claimed the necessity of using the measured single-phase flow Ergun coefficients for the packing of interest. The final form of Sweeney's model contained no parameters adjusted to fit two-phase flow data.

Specchia and Baldi (1977) modeled the gas phase pressure drop by reducing the pore volume and increasing the particle size due to the presence of liquid holdup. Phase interaction was considered negligible in the trickle flow regime. They recommended that Ergun equation coefficients be determined in a bed containing some residual static liquid holdup. A separate correlation was proposed for dynamic liquid holdup, which was not based on the Ergun equation, but did require the pressure gradient calculated from the gas phase momentum balance. In the final form, the model required four parameters adjusted to fit two-phase flow data and a measured value of the static holdup.

Sáez and Carbonell (1985) modified the Ergun equation using empirical correlations for liquid holdup. The method is loosely based on the concept of relative permeability which is used in multiphase flow in consolidated porous media. The momentum balances for the gas and liquid were used in the model with no considerations of phase interaction. The large error associated with using universal Ergun equation coefficients was overlooked and the remedy apparently achieved by adjusting the power dependence of relative permeabilities on holdup. The final form of the model contains two parameters, the power law exponents of the gas and liquid relative permeability functions, which are fitted to two-phase flow data. The additional knowledge of static liquid hold is also required by this model.

Flow regime transition in cocurrent two-phase downflow

Gas and liquid flowing downward in packed beds compete for the void space. This results in various flow regimes, all of which can broadly be divided in two basic categories: low interaction regime (for example, liquid holdup and texture is not affected by changes in gas flow rate) and high interaction regime (for example, changes in gas flow rate affect liquid structure and flow). The low interaction regime, characterized by continuous gas phase and liquid rivulets and/or films, is also called trickle flow regime. Many different flow patterns are identified in the high interaction regime (for example, pulsing, wavy, dispersed bubble, spray, and so on) and distinction is made between foaming and nonfoaming liquids (Ramachandran and Chaudhari, 1983).

The most common method for detecting flow regime transition involves the observation of the flow pattern through transparent column walls. The subjective nature of this qualitative method has resulted in the variety of names reported for the different flow regimes and the uncertainty in flow regime boundaries. A graphical presentation of data in the form of flow regime maps is useful considering the lack of a generally accepted theory regarding the mechanism of the various transitions (Midoux et al., 1976; Talmor, 1977; Fukushima and Kusaka, 1977a, 1978). Talmor (1977) pointed out that the mechanism of transition between each flow regime is expected to be different and no single choice of general flow map coordinates will collapse all transition zones into sharp boundaries. Considering this limitation of flow regime maps, more recent work attempts to develop a fundamental theory of flow regime transition (Sicardi et al., 1979, 1980; Blok et al., 1983; Ng, 1986; Grosser et al., 1988). The majority of the work has focused on the transition from the trickle to pulsing regime which is considered to be of industrial importance.

Sicardi et al. (1979) were the first to attempt to relate a pore-scale phenomenon to the onset of bed scale pulsing. Initially, an analogy was assumed between the onset of pulsing in trickle beds and the initiation of large, turbulent waves in open tubes with cocurrent downflow of air and water. This resulted in an expression which predicted a constant, critical liquid holdup at the transition to pulsing. The data did not support this prediction which was then attributed to the absence of any effect of packing geometry and liquid surface tension in the transition criterion. In a later article (Sicardi and Hoffmann, 1980), a constricted channel model was used to include these effects. A correlation was developed between pressure drop, liquid holdup, liquid surface tension, bed porosity, and particle surface area per unit solid volume at the onset of pulsing. The correlation parameters were determined from flow regime transition data and found to be relatively constant for air-water systems on a variety of packing geometries. The effect of surface tension and liquid viscosity variations were not thoroughly investigated. The resulting empirical criterion for the onset of pulsing can only be considered valid for the air-water system at atmospheric pressure.

Ng (1986) developed criteria to predict transitions between five different flow regimes which have been commonly recognized in trickle beds (trickle, pulse, spray, bubble, dispersed bubble). The trickle to pulsing flow regime boundary is based on a phenomenological analysis of a constricted pore at the point when the liquid first blocks the opening. The resulting model was shown to be in quantitative agreement with the data of Sato et al. (1973b) and Midoux et al. (1976) for air-water systems. However, the model only qualitatively predicted the trends observed by Chou et al. (1977) with changing surface tension and bed porosity.

Blok et al. (1983) conducted an experimental investigation into the hydrodynamic characteristics of the pulsing flow regime. For air-water and water/glycerol solutions with surface tensions between 49 and 72 dyne/cm, they determined that the transition from trickling to pulsing flow occurred at a constant liquid Froude number which was based on the interstitial liquid velocity (superficial velocity/liquid holdup). The value of the critical Froude number is not constant for all liquids. The kinematic liquid viscosity was found to have strong effect, and the liquid surface tension (over the narrow range studied) a negligible effect on the value of the critical liquid Froude number. Other experimental studies have shown the liquid surface

tension to be important in determining the transition to pulsing (Midoux et al., 1976; Chou et al., 1977; Tosun, 1984). No reliable criteria for the transition to pulsing were developed due to the absence of the effect of surface tension in the results.

Grosser et al. (1988) predicted the transition from low to high interaction flow regime by considering a bed scale hydrodynamic model for the low interaction flow regime. Two approaches were presented. The first criterion (their Model I) was developed from a linear stability analysis of the steady-state momentum equations for the gas and liquid in uniform distribution while considering the gas as an incompressible fluid. Loss of stability was interpreted as transition to pulsing. The second method (their Model II) considers the gas to be compressible. Pulsing is assumed to occur at conditions that lead to the loss of existence of a numerical solution to the one-dimensional momentum equations for the gas and liquid with uniform phase distribution. The gas density gradient along the bed axis in the principle flow direction was calculated from predicted pressure gradients and an assigned outlet pressure of the bed. Both criteria use the hydrodynamic models of Saéz and Carbonell (1985) and the capillary pressure curves for porous media where viscous and capillary forces are dominant (that is, sandstone, sand, powders, and so on). The hydrodynamic model of Saéz and Carbonell contains two parameters fitted to two-phase flow data and requires a knowledge of the static liquid holdup. The capillary pressure curve, known as the Leverett J function (Sheideggar, 1957), has not been shown to be applicable in packed beds of particles in the size range typical in trickle bed reactors. The second criterion, based on the existence of the steady-state solution to the one-dimensional momentum balance, gave poor agreement with the data of Chou et al. (1977). The first criterion, based on a linear stability analysis of the one-dimensional steady-state momentum balance, predicted the data of Chou et al. (1977) to within experimental error for air-water systems at several packing porosities, but did not adequately represent the results for changing liquid surface tension. Both criteria predict transition curves for air-water systems which lie within the broad transition zone for the low to high gas-liquid interaction regime on a flow regime map based on Baker (1954) coordinates.

The above studies indicate that besides dimensional analysis and empirical correlations, two basic approaches can be used to model two-phase flow hydrodynamics in packed beds. On the most fundamental level, one can start with the point equations of flow for each phase and use volume averaging to establish a bed scale model. Currently, insufficient information is available to quantify the phase interaction terms which arise in the resulting volume averaged equations. On the other hand, one can use a phenomenological approach to model two-phase flow in a ideal void configuration, and then map the average bed properties to the assumed geometry. Such a phenomenological approach is used in this study to develop a model for the case of uniform phase distribution in the low interaction or trickle flow regime. To be useful, the model should not contain constants that may reflect phase maldistribution. The model should allow us to examine the effect of various variables on a rational basis. Once confirmed by data, such a model should be useful in identification of nonideal flow patterns. Geometric constants which can be determined from single phase (gas) flow experiments are included in such a phenomenological model to characterize the structure and properties of the packed beds. Thus, this study explores the limits and usefulness of a pore scale phenomenological model in prediction of bed scale phenomena.

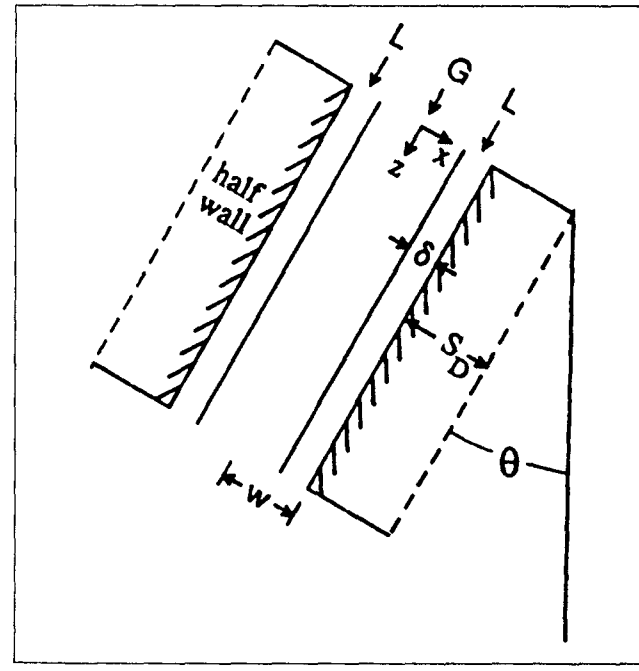

Figure 1. Geometry and phase distribution in a single slit.

Model Development for Pressure Drop and Liquid Holdup Prediction

Geometric model of the bed

The complex geometry of the actual void space in a packed bed of particles is, as an approximation, represented at the pore level by a single, flat walled slit of average half width, w, half wall thickness, S_D, and angle of inclination, θ, to the vertical axis (Figure 1). In the case of saturated single phase flow, the fluid occupies the whole slit. For unsaturated single or two phase flow, the liquid is assumed to completely wet the wall with a film of uniform thickness, δ, while the gas is in the central core. The variables describing the slit geometry can be related to the bed porosity, ϵ, the mean spherical particle diameter, D_p, and the liquid holdup, ϵ_L. We require that the void to solid and liquid to solid volume ratios be the same in the slit and the bed which yields Eqs. 1a and 1b. Additionally, we require the solid volume per unit solid surface area to be the same in both systems which results in Eq. 1c.

$$\frac{w}{S_D}=\frac{\epsilon}{1-\epsilon} \tag{1a}$$

$$\frac{\delta}{S_D}=\frac{\epsilon_L}{1-\epsilon} \tag{1b}$$

$$S_D=\frac{D_p}{6} \tag{1c}$$

We also require the mean intrinsic phase velocities to be the same in the bed and in the representative slit geometry, that is:

$$\langle v_L \rangle \cos\theta = \frac{V_L}{\epsilon_L} \tag{2a}$$

$$\langle v_G \rangle \cos\theta = \frac{V_G}{\epsilon - \epsilon_L} \tag{2b}$$

where $\langle v_\alpha \rangle$ indicates the average velocity of the α phase in the slit and V_α is the superficial velocity of the α phase in the bed. Finally, we require that the total pressure gradient of each phase is the same in the bed and the representative slit.

$$\frac{1}{\cos\theta}\left(-\frac{dP}{dz} + \rho_\alpha g_z\right) = -\frac{\Delta P}{L_{\text{bed}}} + \rho_\alpha g \tag{3}$$

The angle of inclination of the slit from vertical defines the bed tortuosity

$$T = \frac{1}{\cos\theta} \tag{4}$$

which represents the ratio of the actual distance traveled by the fluid to the vertical length of the bed. Equations 1 to 4 are the relationships required to relate the hydrodynamics in a simple flat walled slit to the bed scale.

Single-phase flow model

We first show that the Ergun equation results from this representative slit geometry in the case of saturated single-phase flow. The single-phase flow model can be developed based on only average velocities, but the two-phase flow model requires a velocity profile in order to determine the interfacial velocity. We use the universal velocity profile as a common basis in all model development. Furthermore, we use the linear velocity profile usually associated with the laminar sublayer in a turbulent core to describe laminar liquid flow in the slit. This assumption can be justified by the physical argument that the natural bed tortuosity, that is, the change of inclination θ that happens on the order of every particle diameter in a real bed, prevents the fully developed, parabolic laminar velocity profile from being established and makes the linear form a reasonable first approximation. One can also argue that the dribbling (that is, sudden acceleration and deceleration) of the liquid down the bed in a time averaged sense is better described with a linear than parabolic velocity profile.

One can show that the integrated form of the universal velocity profile can be represented over a range of slit Reynolds numbers, Re'_α, by an Ergun like expression with an appropriate choice of the wall friction factor, f_{wall} (Holub, 1990).

$$\frac{\tau_{\text{wall}} w^2 \rho_\alpha^2}{\mu_\alpha^2} = 2\,Re'_\alpha + f_{\text{wall}} Re'^2_\alpha \tag{5}$$

A force balance on the fluid in the slit gives the relationship between the wall shear stress and the total pressure gradient:

$$\tau_{\text{wall}} = \left(-\frac{dP}{dz} + \rho_\alpha g_z\right) w \tag{6}$$

We eliminate the wall shear stress in Eq. 5 using Eq. 6 and substitute Eqs. 1 through 4 to obtain the appropriate form of Eq. 5 in terms of bed variables. Upon rearrangement into dimensionless groups, the following equation is obtained which relates the bed pressure drop and flow rate of the single flowing phase α:

$$\Psi_\alpha = \frac{E_1 Re_\alpha}{Ga_\alpha} + \frac{E_2 Re_\alpha^2}{Ga_\alpha} \tag{7}$$

Here, $E_1 = 72T^2$, $E_2 = 6T^3 f_{\text{wall}}$, and $\Psi_\alpha = -[\Delta P/L + \rho_\alpha g]/\rho_\alpha g$. We recognize Eq. 7 as the Ergun equation which is customarily presented in the following dimensional form:

$$-\frac{\Delta P}{L_{\text{bed}}} + \rho_\alpha g = \frac{E_1 \mu_\alpha (1-\epsilon)^2}{D_p^2 \epsilon^3} V_\alpha + \frac{E_2 \rho_\alpha (1-\epsilon)}{D_p \epsilon^3} V_\alpha^2 \tag{8}$$

As recommended by MacDonald et al. (1979), the constant E_1 and E_2 should be determined for each packing of interest since the use of the "universal Ergun constants" of $E_1 = 150$ and $E_2 = 1.5$ can lead to errors in the pressure drop prediction of several hundred percent. Finally, one should note that upon integration of the velocity profile, as done to obtain Eqs. 5 and 7, the difference between the assumed linear or parabolic profile for laminar flow results in a different numerical constant which is ultimately incorporated into E_1. Hence, the assumption of the linear profile can be made for simplicity with no change in the final form of Eqs. 7 and 8.

Two-phase flow model of the trickle flow regime

To develop the modified form of the Ergun equation for two-phase flow, we make the following additional assumptions:

- Symmetric, steady liquid film flow of constant film thickness in the slit. Actually liquid moves also in discrete packets in a chaotic manner and a steady film thickness is used in a time averaged sense to assure a simple model.
- Universal velocity profile holds in the liquid film and gas core (Dukler and Bergelin, 1952; Pike, 1965). The linear representation of the laminar film velocity profile is more applicable than the fully developed parabolic profile for the transient, discrete packets of liquid.
- Interfacial friction factor is equal to the wall friction factor. This is reasonable for a smooth wall and smooth interface, see Hanratty and Engen (1957), but is only an approximation when wall roughness dominates the interface structure.

Finally, in order to compensate for the idealization of the real situation by the model, we allow for a possible discontinuity in velocity and shear at the gas-liquid interface by introducing two proportionality constants, f_v and f_s, such that:

$$v_{i,G} = f_v v_{i,L} \tag{9a}$$

$$\tau_{i,L} = f_s \tau_{i,G} \tag{9b}$$

The values of f_v and f_s have some physical significance in the slit model in terms of the velocity profiles in the gas and liquid at the interface. If both f_v and f_s are equal to one, then a continuity condition for both velocity and shear is satisfied at the interface. If both f_v and f_s are zero, then no interaction occurs between the gas and liquid at the interface. Negative values for f_v and f_s could indicate the presence of recirculation cells at the gas-liquid interface and exertion of shear by one phase on the other. Due to the simple, flat film model used, no exact information on the interfacial condition can be obtained by matching model predictions to data in terms of adjusting f_v and f_s. The above explanations provide only a qualitative insight into a very complex situation. As already discussed, we recognize that the above simplifying assumptions do not fully reflect the physical reality at any instant in any void of the bed since the liquid has been observed to have a dribbling as well as a film flow pattern. However, our goal is to model the average or macroscopic bed behavior. In that sense, we believe that the above assumptions lead to a better model than assuming fully developed laminar films with parabolic velocity profiles. Ultimately, our assumptions are justified if they lead to a useful result.

The two-phase flow momentum balance for the slit, coupled with the use of the universal velocity profile and above cited assumptions, takes the form of an Ergun like expression for the gas and the liquid given by Eqs. 10 and 11. Details are reported by Holub (1990).

$$\frac{\tau_{i,G}(w-\delta)^2\rho_G^2}{\mu_G^2}=2\left(\frac{w-\delta}{w}\right)(Re_G'-f_vRe_{i,L}')+f_{\text{wall}}\left(\frac{w-\delta}{w}\right)^2(Re_G'-f_vRe_{i,L}')^2 \quad (10)$$

$$\frac{\tau_{\text{wall}}\delta^2\rho_L^2}{\mu_L^2}=2\left(\frac{\delta}{w}\right)Re_L'+f_{\text{wall}}\left(\frac{\delta}{w}\right)^2Re_L'^2 \quad (11)$$

where

$$Re_{i,L}'=\frac{\tau_{\text{wall}}\delta w\rho_L}{\mu_L^2}$$

if

$$\sqrt{\frac{\tau_{\text{wall}}}{\rho_L}}\left(\frac{\delta\rho_L}{\mu_L}\right)\le 5$$

$$Re_{i,L}'=\sqrt{\frac{\tau_{\text{wall}}}{\rho_L}}\left(\frac{w\rho_L}{\mu_L}\right)\left[-3.05+5\ln\left(\sqrt{\frac{\tau_{\text{wall}}}{\rho_L}}\left(\frac{\delta\rho_L}{\mu_L}\right)\right)\right]$$

$$\text{if}\quad 5<\sqrt{\frac{\tau_{\text{wall}}}{\rho_L}}\left(\frac{\delta\rho_L}{\mu_L}\right)\le 30$$

$$Re_{i,L}'=\sqrt{\frac{\tau_{\text{wall}}}{\rho_L}}\left(\frac{w\rho_L}{\mu_L}\right)\left[5.5+2.5\ln\left(\sqrt{\frac{\tau_{\text{wall}}}{\rho_L}}\left(\frac{\delta\rho_L}{\mu_L}\right)\right)\right]$$

$$\text{if}\quad \sqrt{\frac{\tau_{\text{wall}}}{\rho_L}}\left(\frac{\delta\rho_L}{\mu_L}\right)>30$$

Table 1. Two-Phase Flow Hydrodynamic Model for the Low Interaction Regime

$$\Psi_G=\left(\frac{\epsilon}{\epsilon-\epsilon_L}\right)^3\left[\frac{E_1(Re_G-f_v(\epsilon-\epsilon_L)Re_i)}{Ga_G}+\frac{E_2(Re_G-f_v(\epsilon-\epsilon_L)Re_i)^2}{Ga_G}\right] \quad (T1)$$

$$Re_i=\frac{V_{i,L}D_p}{\nu_G(1-\epsilon)} \quad (T2)$$

$$\Psi_L=\left(\frac{\epsilon}{\epsilon_L}\right)^3\left[\frac{E_1Re_L}{Ga_L}+\frac{E_2Re_L^2}{Ga_L}\right]+f_s\left(\frac{\epsilon-\epsilon_L}{\epsilon_L}\right)\left(1-\frac{\rho_G}{\rho_L}-\Psi_L\right) \quad (T3)$$

$$Re_i=\Phi\eta_L \qquad 0<\eta_L<5 \quad (T4)$$

$$Re_i=\Phi(-3.05+5\ln\eta_L) \qquad 5<\eta_L<30 \quad (T5)$$

$$Re_i=\Phi(5.5+2.5\ln\eta_L) \qquad \eta_L>30 \quad (T6)$$

$$\Phi=\frac{10}{(E_1)^{0.75}}\frac{\nu_L}{\nu_G}\sqrt{\frac{\epsilon_L}{\epsilon^3}\Psi_LGa_L\left(1+f_s\frac{\epsilon-\epsilon_L}{\epsilon_L}\frac{\rho_G}{\rho_L}\frac{\Psi_G}{\Psi_L}\right)} \quad (T7)$$

$$\eta_L=\frac{1}{5(E_1)^{0.25}}\sqrt{\left(\frac{\epsilon_L}{\epsilon}\right)^3\Psi_LGa_L\left(1+f_s\frac{\epsilon-\epsilon_L}{\epsilon_L}\frac{\rho_G}{\rho_L}\frac{\Psi_G}{\Psi_L}\right)} \quad (T8)$$

$$\Psi_L=1+\frac{\rho_G}{\rho_L}(\Psi_G-1) \quad (T9)$$

A force balance on the gas core and liquid film in the slit yields, respectively:

$$\tau_{i,G}=\left(-\frac{dP}{dz}+\rho_Gg_z\right)(w-\delta) \quad (12)$$

$$\tau_{\text{wall}}=\tau_{i,L}+\left(-\frac{dP}{dz}+\rho_Lg_z\right)\delta \quad (13)$$

Using Eqs. 9b, 12, and 13, we get the relationship between the pressure gradient and the wall shear.

$$\tau_{\text{wall}}=\left(-\frac{dP}{dz}+\rho_Lg_z\right)(\delta+f_s(w-\delta))-f_s(w-\delta)(\rho_L-\rho_G)g_z \quad (14)$$

Substituting Eqs. 1 to 4 into Eqs. 10 to 14 and rearranging into the appropriate dimensionless groups gives the two-phase flow model for the packed bed. The complete model is given in Table 1. The dimensionless gas and liquid pressure gradients, Ψ_G and Ψ_L, are given in terms of the phase Reynolds and Galileo numbers, the phase holdups, an interfacial Reynolds number, and the parameters, f_v and f_s, which characterize the degree of phase interaction at the gas-liquid interface. Equation T9 in Table 1 is an implicit equation in liquid holdup formed by equating the dimensional pressure gradient in the gas and liquid. This equation reflects the assumption of uniform phase distribution in the bed which implies a zero capillary pressure gradient. The model in Table 1 is a two-phase flow form of the Ergun equation containing two-phase interaction param-

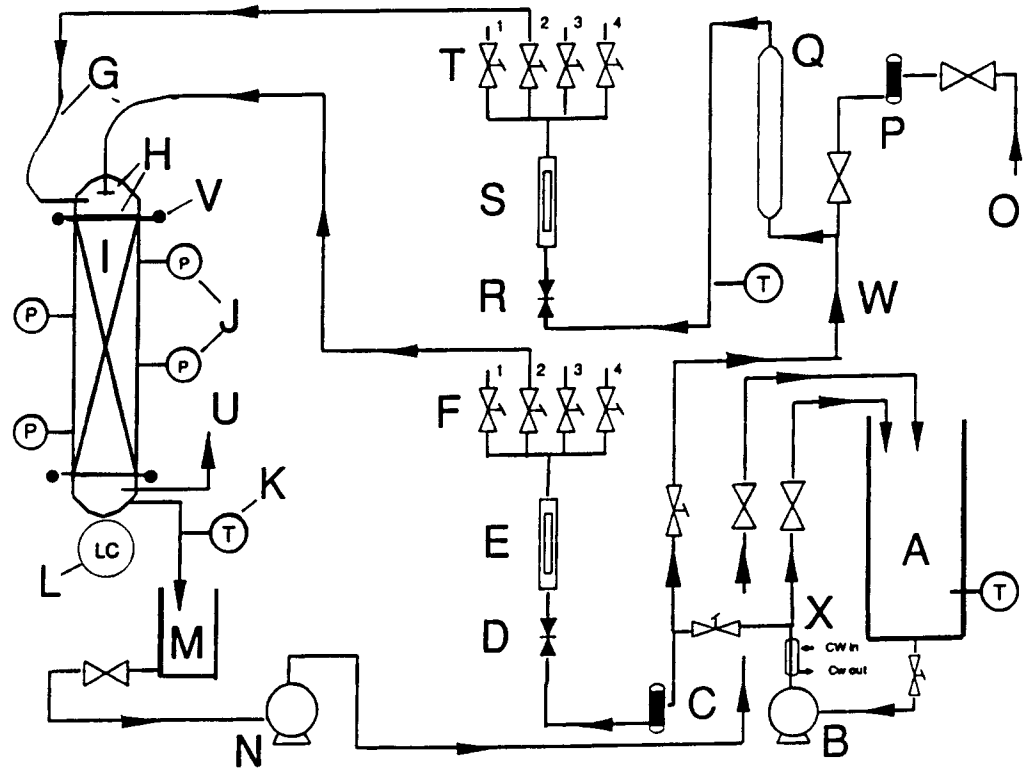

A. Liquid feed tank
B. Liquid feed pump
C. Liquid filter
D. Liquid flow control valve
E. Liquid rotameters (5)
F. Liquid shutoff valves for column selection
G. Flexible hose connectors
H. Liquid distributors, spray head and orifice plate
I. Column 2 (3.125 inch I.D., 2 feet long)
J. Pressure transducers
K. Thermocouple
L. Load cell to weigh column
M. Receiving tank
N. Liquid recycle pump
O. House air, 120 psig
P. Air trap
Q. Air humidifier
R. Air flow control valve
S. Air rotameters (5)
T. Air shutoff valves for column selection
U. Air exhaust to room
V. Column supported in tracks for free vertical movement
W. Liquid feed line for gas saturator.
X. Heat Exchanger to cool liquid feed to room temperature

Figure 2. Experimental apparatus.

eters, f_v and f_s, which must be determined from experimental data.

Experimental Database

To test the developed model, an extensive experimental database was developed by performing pressure drop and liquid holdup measurements in our laboratory and by acquiring data from the literature. Only those data that reflect uniform liquid distribution in the low interaction regime are included in the database. This means that the beds were brought to the desired operating point in the low interaction regime from the high interaction regime thus assuring operation on the upper branch of the pressure drop hysteresis loop, indicating uniform liquid distribution (Levec et al., 1986, 1988; Christensen et al., 1986; Lazzaroni et al., 1989). All operating points were in the low interaction regime as indicated by all flow maps.

A schematic diagram of the experimental apparatus used for pressure drop and liquid holdup measurements is shown in Figure 2. For all runs, the gas and liquid phases were at room temperature (approximately 24°C). The outlet of each column is at atmospheric pressure. Any heat generated by pumping the liquid was removed with a heat exchanger. The gas was saturated with the liquid phase before entering the column to avoid evaporation. For each gas and liquid flow rate, ample time (usually a minimum of about 15 min) was allowed for the pressure drop and liquid holdup measurements to become constant indicating steady state. Several tests were conducted over longer times (4 to 8 h) to ensure the data reflected true steady states. Low to high interaction flow regime transition data was also obtained as a result of the operating procedures used to ensure uniform phase distribution.

Three different beds (Table 2) were used. Liquid distribution was accomplished with spray heads followed by orifice plates in the larger columns. The orifice plates were constructed to give one distribution point per square centimeter. The one in. columns used only a spray head distributor. A uniform distribution was further ensured by bringing the bed first to a high

Table 2. Physical Characteristics of Available Beds

Bed	Inside Dia. in. (mm)	Total Length ft (m)	Type of Liquid Distributor	No. of Pres. Taps	Material of Construction
1	5⅝ (142 mm)	6 (1.9 m)	Spray head + orifice plate	5 along bed	Plexiglass
2	3⅛ (79 mm)	2 (0.6 m)	Spray head + orifice plate	4 along bed	Plexiglass
3	1 (25 mm)	1.5 (0.5 m)	Spray head	1 at bed inlet	Glass

interaction regime at a given gas flow rate, and then slowly decreasing the liquid flow rate to move into the low interaction regime. The transition from the high to low interaction regime was determined by the cessation of pressure fluctuations characteristic of the pulsing flow regime (Sato et al., 1973b; Chou et al., 1977; Sicardi et al., 1979, 1980; Blok et al., 1983; and Tosun, 1984) or by visual observations of the bed for dispersed bubble flow regimes. This qualitative method for distinguishing the dispersed bubble flow regime is currently the only one reported in the literature. This operating procedure was recommended by Levec et al. (1986, 1988), Christensen et al. (1986), and Lazzaroni et al. (1989) for ensuring uniform liquid distribution based on observations on pressure drop hysteresis. The phenomenon of pressure drop and liquid holdup hysteresis reported by Levec et al. (1986, 1988), Christensen et al. (1986), and Lazzaroni et al. (1989) was observed in our laboratory, but operating histories which include the high interaction flow regimes were used to avoid the phase maldistribution which is present for the lower pressure drops on the hysteresis loop.

Pressure measurements are made with pressure transducers attached to each bed. For beds 1 and 2, the pressure is measured at several locations along the bed length. The pressure gradient remained constant along the bed length below the entry region (approximately a column diameter in length) as was reported by Specchia and Baldi (1977) and Sato et al. (1973a). For bed 3 the packing support is a low porosity screen and the bed outlet is open to the atmosphere so that the bed pressure drop can be measured with a single transducer. For beds 1 and 2, the pressure drop was measured between the transducers immediately below the entry region and just above the support plate. For bed 3, the pressure drop was measured across the entire bed length and included the effect of the entry region and the support screen. The design of bed 3 included a large length to diameter ratio of 24 and a low porosity support screen to minimize the error associated with these end effects.

Liquid holdup measurements are made by the weighting method using strain gauge load cells. The weighing method is recommended by Levec et al. (1986) and Sato et al. (1973a). Liquid holdup is calculated by the increase in weight over the dry bed when liquid is flowing. Calibration runs for the holdup of the apparatus were conducted without the packing in place. All runs were carried out at room temperature and near atmospheric pressure. The single-phase flow Ergun equation coefficients were determined from pressure drop measurements using gas flow over dry packing of interest. Runs for liquid film flow in stagnant gas were conducted by decreasing the liquid flow rate from the flooding point. The flooding point was determined visually when liquid accumulates in the top of the column.

Two-phase flow runs were performed over a range of gas and liquid flow rates spanning the low interaction or trickle flow regime. A summary of the data gathered in this work and the data obtained from other investigators is presented in Tables 3 and 4. Figure 3 shows the range of Reynolds numbers covered by the data in Table 3. The flow regime transition lines of Fukushima and Kusaka (1977a) are shown for reference.

All data in our database meet the previously described criteria that uniform liquid distribution was present in the bed. The data of Anderson (Mobil Oil Corp.) and Levec et al. (1986) reflect the same operating conditions used in this work to ensure uniform liquid distribution. The raw data obtained from Specchia and Baldi (1977) indicate that a similar operating procedure was followed in their experiments. The resulting database consists of 320 data points spanning the following fluid physical property and bed property ranges ($920 \le \rho_L \le 1{,}070$ kg/m^3; $1.2 \le \rho_G \le 2.4$ kg/m^3; $100 \le E_1 \le 850$; $0.01 \le \mu_L \le 0.57$ poise; $\mu_G = 1.8 \times 10-4$ poise; $0.8 \le E_2 \le 2.7$; $0.027 \le \sigma_L \le 0.072$ N/m; $1.8 \times 10^{-3} \le D_p \le 6.0 \times 10^{-3}$ m; $0.335 \le \epsilon \le 0.45$).

Comparison of Model Predictions for Pressure Drop and Liquid Holdup and Data

Two-phase flow

The developed model contains two unknown parameters, f_v and f_s, reflecting the lack of a reliable simple model for the gas-liquid interface. We now compare model predictions and data for pressure drop and liquid holdup for different values of f_v and f_s. A pattern search was done over the ranges -1 to $+1$ to show the sensitivity of the model to f_v and f_s and determine the values which minimize the error. For a given pair of f_v and f_s values, the mean relative error between the predicted and experimental pressure drop and liquid holdup values was calculated by:

$$\hat{e}_\phi = \frac{1}{N}\sum_{i=1}^{N} \frac{|\phi_{\text{predicted}} - \phi_{\text{experimental}}|}{\phi_{\text{experimental}}} \tag{15}$$

where the predicted values were obtained by solving the model equations in Table 1 and the experimental values are those summarized in Table 3 ($N = 320$). The mean relative error in dimensionless gas phase pressure gradient as a function of f_v and f_s is shown in Figure 4. The corresponding diagram for the total liquid holdup is shown in Figure 5. Figures 4 and 5 reveal that minimum error in pressure drop and holdup does not occur at the same values of f_v and f_s. However, both the pressure drop and liquid holdup data (Figures 4 and 5) indicate that f_v and f_s can both be chosen as zero with only a small

Table 3. Two-Phase Flow Data: Pressure Drop, Liquid Holdup and Single-Phase Ergun Equation Constants

Symbol	Packing Description	D_p mm	Gas-Liquid System*	Dc/D_p	Bed Prop. $E_1/E_2/\epsilon$	Source	No. of Points
◇	Glass spheres	3	Air-Water	26.5	215/1.4/0.375	This Work	34
•	1/16th in. Nalco HDS extrudates[2]	1.88	Air-Water	13.5	100/0.8/0.335	This Work	25
▽	Glass spheres	3	Air-Water	51.0	215/1.4/0.375	Levec (1986)	50
■	Porous Al_2O_3 spheres	3.175	Air-Water-Isopropanol (10%)†	12.0	140/0.8/0.35	D. H. Anderson Mobil Oil Co.	40
+	Glass spheres	6	Air-Water	13.3	850/2/0.4	G. Baldi (1977)	8
*	Glass cylinders	2.7	Air-Water	29.6	300/2/0.38	G. Baldi (1977)	11
△	Glass cylinders	5.4	Air-Water	14.8	500/2.4/0.37	G. Baldi (1977)	12
×	Glass Cylinders	5.4	Air-Water-Glycerol (9%)††	14.8	500/2.4/0.37	G. Baldi (1977)	2
○	Glass cylinders	5.4	Air-Water-Glycerol (29%)†††	14.8	500/2.4/0.37	G. Baldi (1977)	1
◍	Glass spheres	3	Air-Soybean Oil††††	26.5	215/1.4/0.375	This Work	37
▲	1/16 in. (1.6 mm) Nalco HDS extrudates**	1.88	Air-Soybean Oil	13.5	100/0.8/0.335	This Work	65
●	Porous Al_2O_3 spheres	3.175	Air-Soybeam Oil	45	270/2.7/0.46	This Work	26

* All systems are at room temperature (22°C) and low pressure (<2 atm).
Air: ρ_G = ideal gas value 1.2 to 2.4 kg/m^3; $\mu_G = 0.018$ cp.
Water: $\sigma_L = 72$ dyne/cm; $\rho_L = 1.0$ g/cm^3; $\mu_L = 1.0$ cp.
** From Nalco catalyst company, Chicago, IL; 1/16 in. (1.6 mm) dia.; $L/D = 2$.
† $\sigma_L = 41$ dyne/cm; $\rho_L = 0.96$ g/cm^3; $\mu_L = 1.1$ cp.
†† $\sigma_L = 52$ dyne/cm; $\rho_L = 1.03$ g/cm^3; $\mu_L = 1.2$ cp.
††† $\sigma_L = 44$ dyne/cm; $\rho_L = 1.07$ g/cm^3; $\mu_L = 2.35$ cp.
†††† $\sigma_L = 27$ dyne/cm; $\rho_L = 0.92$ g/cm^3; $\mu_L = 57$ cp.

increase in error over the observed minimum. The mean relative error in dimensionless gas phase pressure drop is 44% for the air-water based systems and 25% for the air-soybean oil system. The mean relative error in total liquid holdup is 11% for the air-water based systems and 8.6% for the air-soybean oil system.

When $f_v = f_s = 0$ is chosen in Table 1, the resulting model contains no parameters which have to be fitted to two-phase

Table 4. Liquid Holdup Data in the Absence of Gas Flow (Zero Shear): Single-Phase Flow Ergun Equation Constants are from Single-Phase Gas Flow Data

Symbol	Packing Description	D_p mm	Liquid System*	Dc/D_p	Bed Prop. $E_1/E_2/\epsilon$	Source	No. of Points
•	1/16th in. Nalco HDS extrudates**	1.88	Water	13.5	100/0.8/0.335	This Work	16
+	Glass spheres	6	Water	13.3	850/2/0.4	G. Baldi (1977)	5
*	Glass cylinders	2.7	Water	29.6	300/2/0.38	G. Baldi (1977)	4
△	Glass cylinders	5.4	Water	14.8	500/2.4/0.37	G. Baldi (1977)	5
×	Glass cylinders	5.4	Water-Glycerol (9%)†	14.8	500/2.4/0.37	G. Baldi (1977)	4
○	Glass cylinders	5.4	Water-Glycerol (29%)††	14.8	500/2.4/0.37	G. Baldi (1977)	5
◍	Glass spheres	3	Air-Soybean Oil†††	26.5	215/1.4/0.375	This Work	19
▲	1/16th in. Nalco HDS extrudates	1.88	Air-Soybean Oil	13.5	100/0.8/0.335	This Work	9

* All systems are at room temperature and low pressure (<2 atm).
Air: ρ_G = ideal gas value 1.2 to 2.4 kg/m^3; $\mu_G = 0.018$ cp.
Water: $\sigma_L = 72$ dyne/cm; $\rho_L = 1.0$ g/cm^3; $\mu_L = 1.0$ cp.
** From Nalco catalyst company, Chicago, IL; 1/16 in. (1.6 mm) dia.; $L/D = 2$.
† $\sigma_L = 52$ dyne/cm; $\rho_L = 1.03$ g/cm^3; $\mu_L = 1.2$ cp.
†† $\sigma_L = 44$ dyne/cm; $\rho_L = 1.07$ g/cm^3; $\mu_L = 2.35$ cp.
††† $\sigma_L = 27$ dyne/cm; $\rho_L = 0.92$ g/cm^3; $\mu_L = 57$ cp.

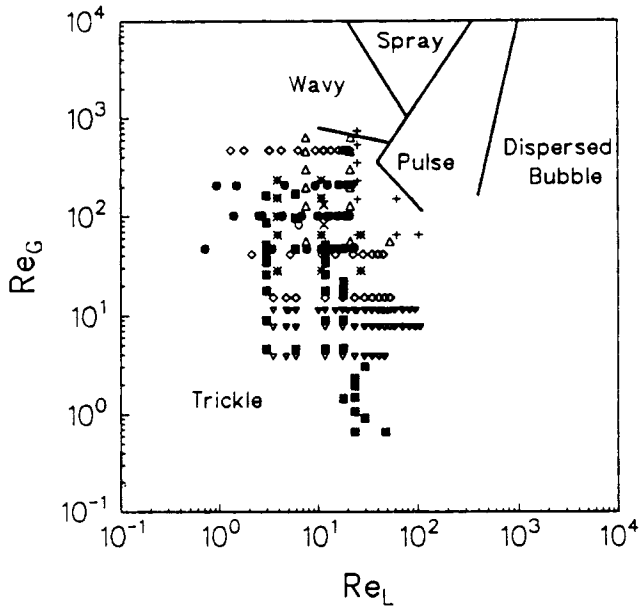

Figure 3. Experimental conditions covered by the data.

Flow regime map proposed by Fukashima and Kusaka (1977) shown for reference.

flow hydrodynamic data, but the single-phase flow Ergun equation coefficients must be determined for each bed to obtain reliable predictions. This simplified model for the trickle flow regime can be summarized by Eqs. 16 to 18.

$$\Psi_G = \left(\frac{\epsilon}{\epsilon - \epsilon_L}\right)^3 \left[\frac{E_1 Re_G}{Ga_G} + \frac{E_2 Re_G^2}{Ga_G}\right] \tag{16}$$

$$\Psi_L = \left(\frac{\epsilon}{\epsilon_L}\right)^3 \left[\frac{E_1 Re_L}{Ga_L} + \frac{E_2 Re_L^2}{Ga_L}\right] \tag{17}$$

$$\Psi_L = 1 + \frac{\rho_G}{\rho_L}(\Psi_G - 1) \tag{18}$$

Equation 18 results from the fact that in uniform two-phase flow, the capillary pressure gradients in the liquid phase are zero. Equations 16 to 18 form a closed system of equations for the pressure gradient and liquid holdup. Sweeney (1967) arrived at this model from empirical arguments, but he did not justify it and made no comparison to liquid holdup data. Figures 6 and 7 compare the predicted values of dimensionless gas phase pressure drop and total liquid holdup with the corresponding data in Table 3. Equations 16 and 17 indicate that relative permeability is proportional to the third power of relative saturation. Sáez and Carbonell (1985) predict different power dependencies possibly because they employed universal values for the Ergun constants. The large departure of these constants from universal values is evident in Table 3.

The resulting pressure drop and holdup model (Eqs. 16–18) indicates a slip in velocity at the gas-liquid interface and zero shear at the interface in the liquid film. This implies that gas

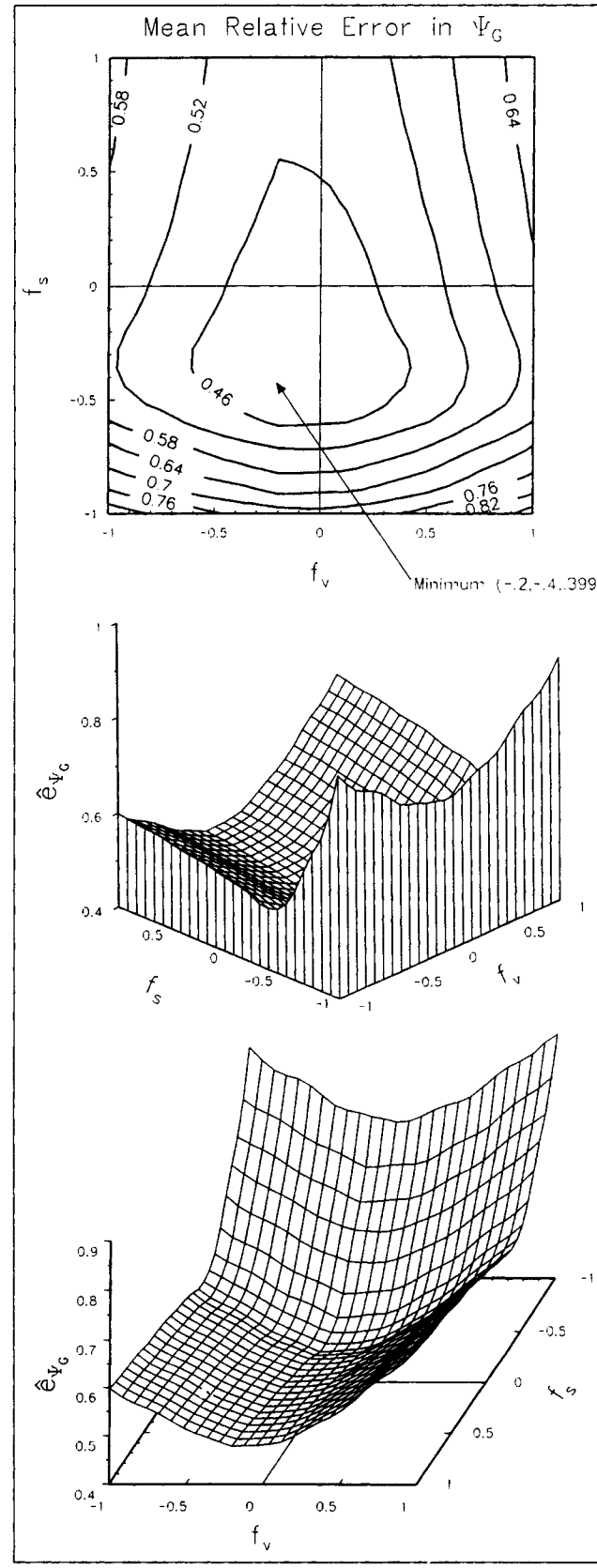

Figure 4. Mean relative error in dimensionless gas pressure drop calculated from the data set in Table 3 for the various values of f_v and f_s.

Three different views of the error surface.

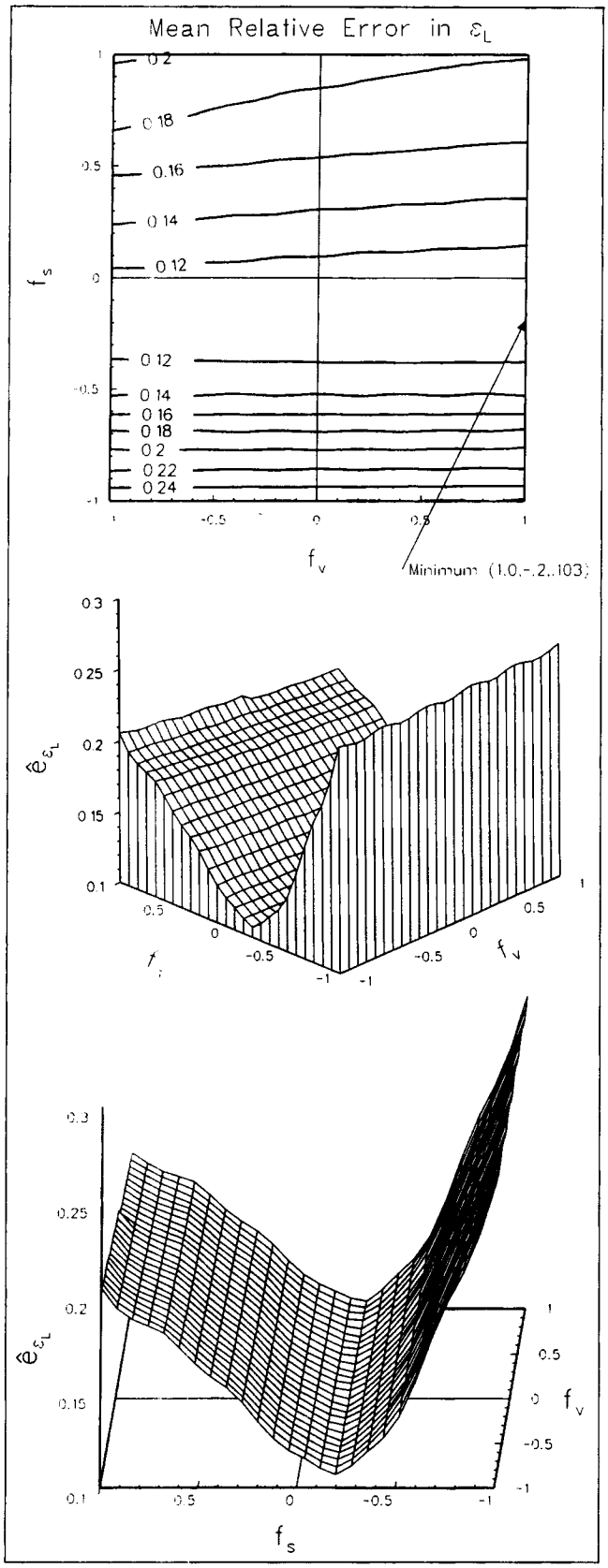

Figure 5. Mean relative error in total liquid holdup calculated from the data set in Table 3 for the various values of f_v and f_s.

Three different views of the error surface.

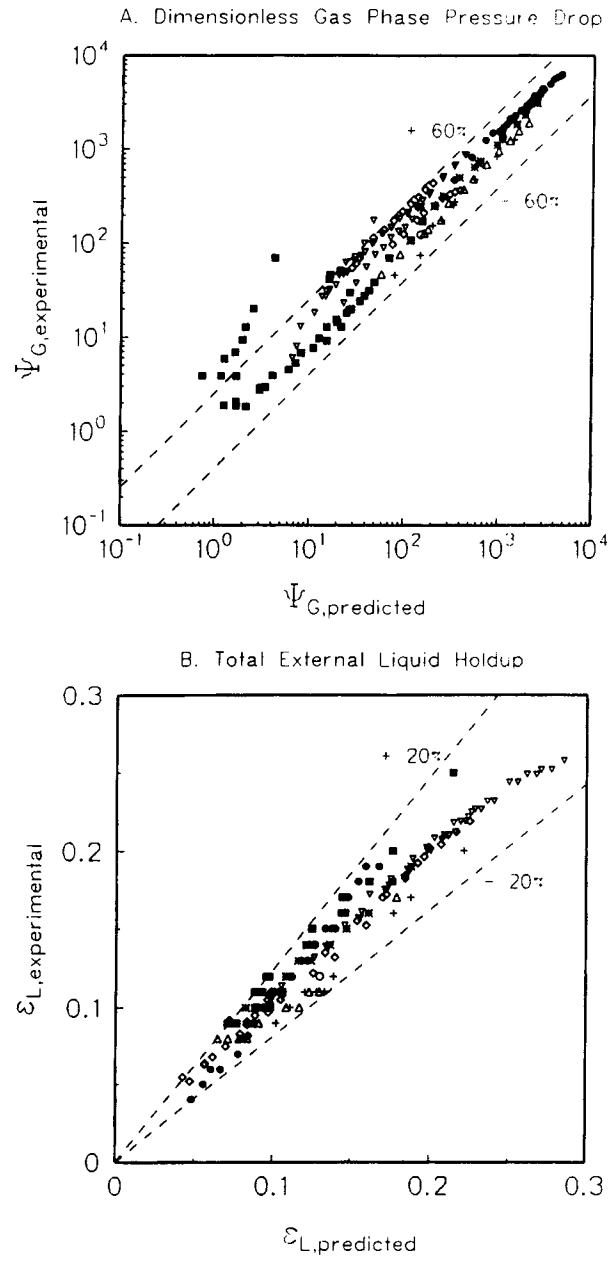

Figure 6. Comparison of model predictions to dimensionless gas-phase pressure drop and total external liquid holdup data for two-phase flow in packed beds with the air-water based systems.

The symbols correspond to the data sets in Table 3.

flow does not affect the liquid, which is a known characteristic of trickle flow. It also implies that a parabolic liquid velocity profile could be used. As mentioned earlier, the use of a parabolic velocity profile for the liquid film would, upon more complicated algebra, yield the same result regarding the pressure drop—Reynolds number relationship. The indicated discontinuity in velocity at the interface can be rationalized considering the approximate representation of the complex liquid film structure by the slit model and by the observed fact that the gas flow does not affect liquid structure.

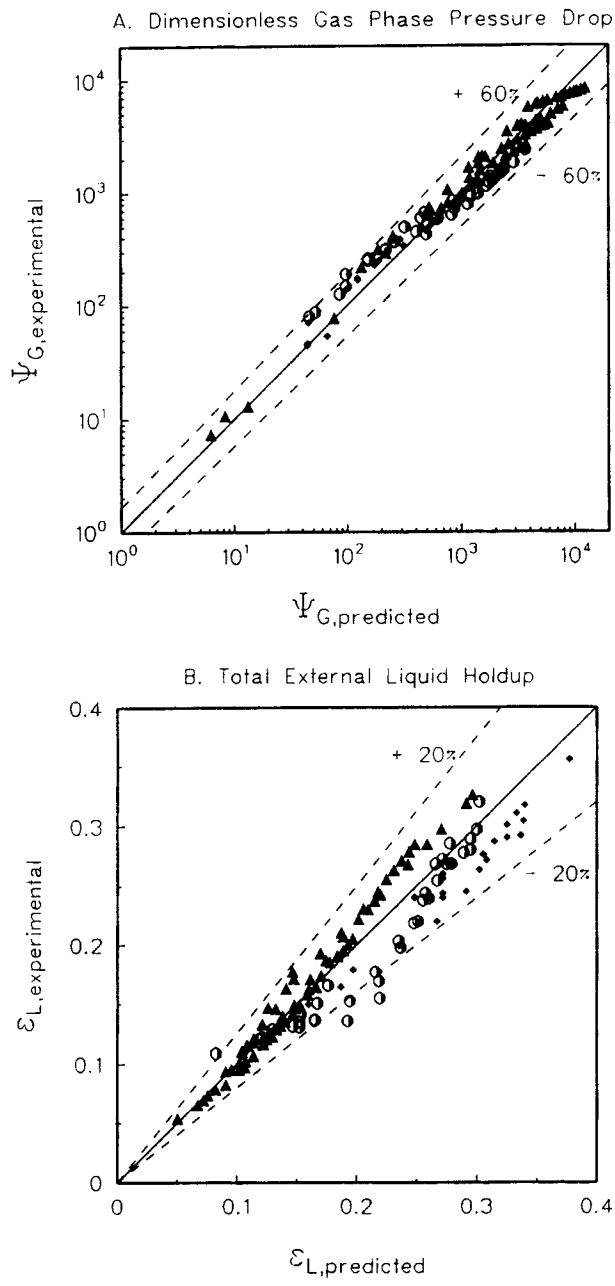

Figure 7. Comparison of model predictions to dimensionless gas-phase pressure drop and total external liquid holdup data for two-phase flow in packed beds with the air-soybean oil system.

The symbols correspond to the data sets in Table 3.

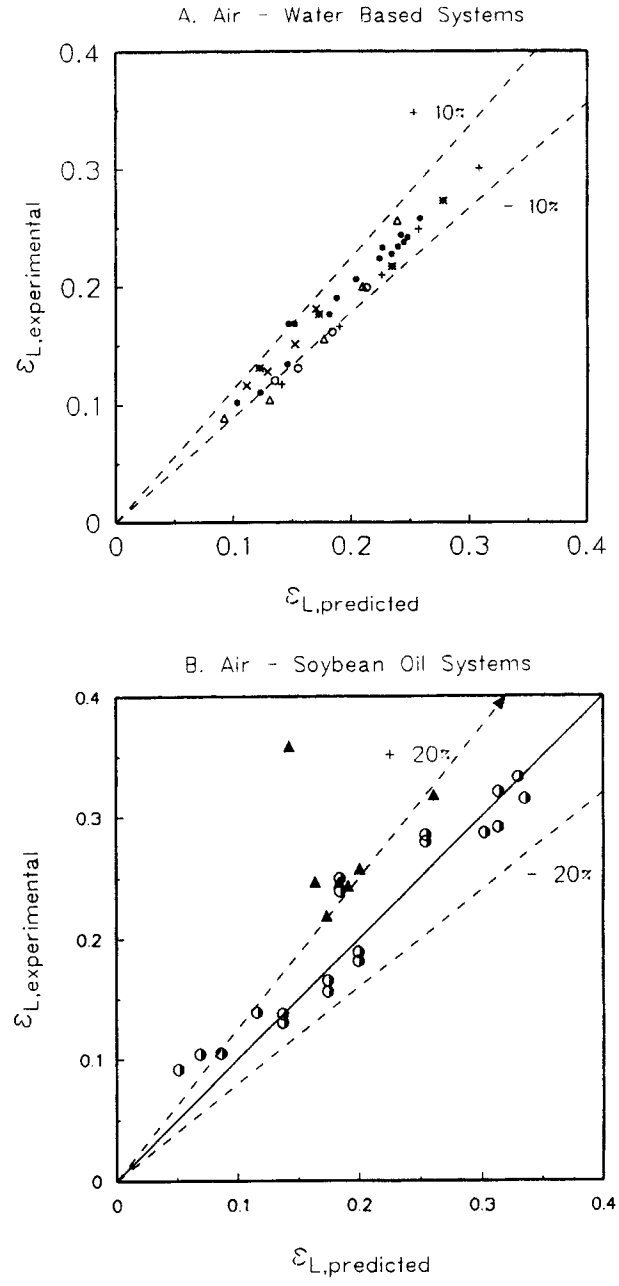

Figure 8. Comparison of model predictions to liquid holdup data for zero gas flow (zero interfacial shear) in packed beds.

The symbols correspond to the data sets in Table 4.

Single-phase unsaturated (liquid film) flow

A subcase of the two-phase flow model in Table 1 is liquid film flow in a stagnant gas. No shear is exerted on the liquid by the gas and flow is due to gravity only. In this case, Eq. T3 reduces to a simple form which contains no adjustable parameters since the bed parameters E_1 and E_2 are determined from single-phase gas flow experiments in dry beds. Equation 19 gives a complete model for liquid holdup under stagnant gas conditions.

$$\left(\frac{\epsilon}{\epsilon_L}\right)^3\left[\frac{E_1 Re_L}{Ga_L}+\frac{E_2 Re_L^2}{Ga_L}\right]=1 \tag{19}$$

A database of 66 total liquid holdup values from the same beds and independent sources used in the two phase flow experiments, as shown in Table 4, gives a mean relative error for total liquid holdup of 6.3% for the water based systems and 11.2% for the soybean oil system. The increased error with the viscous soybean oil is due to difficulties in obtaining uniform distribution in our apparatus in the absence of gas

flow. Figure 8 compares the total liquid holdup predictions with the corresponding data in Table 4.

Flow Regime Transition

Model development

The success of our pore scale phenomenological model of the trickle flow regime indicates that liquid films can be considered laminar with negligible interfacial shear due to the flowing gas. The loss of laminar film stability can then be considered as a mechanism of transition from the low to high interaction flow regime. Kapitza's (1945) criterion for the onset of interfacial waves on laminar liquid films was thus applied to the slit model and then mapped to the bed scale using Eqs. 1 to 4 (Holub, 1990). Kapitza's development assumes parabolic velocity profiles in laminar liquid films along a inclined plane. Such a parabolic velocity profile is quite compatible with Eqs. 16 to 18 as mentioned earlier and as shown by Holub (1990). Kapitza's (1945) criterion in terms of bed variables requires that inequality in Eq. 20a be satisfied for the existence of nonwavy films, that is, for the existence of the low interaction regime. The condition in Eq. 20b arises due to the assumption made in the development of Eq. 20a that the wavelength of the disturbance must be *much greater* than the film thickness. Kapitza only required that the film equivalent of the lefthand side of Eq. 20b be much greater than one; we found that most of the data satisfy a limit simply greater than three. Inequality in Eq. 20c arises in the inherent assumption that the films are laminar prior to transition. This places an upper bound on film thickness. We found that using $\eta_L < 6$ (see Eq. T4) identifies the conditions when viscous forces are dominant in the liquid film. With the mapping to bed variables and experimentally measured single-phase flow Ergun constants, Kapitza's criterion for the onset of waves, as presented in Eq. 20, contains no empirical parameters (E_1 is determined by single-phase flow experiments).

$$\frac{Re_{L,\text{critical}} \Psi_L^{1/11} E_1^{5/11}}{25\, Ka^{1/11}} \leq 1 \tag{20a}$$

$$0.49\, E_1^{1/22} \left(\frac{Ka}{\Psi_L}\right)^{1/11} > 3 \tag{20b}$$

$$Re_L < \frac{900}{\sqrt{E_1}} \tag{20c}$$

Database for flow regime transition

A database for the transition from low to high interaction regime was compiled from data obtained in our laboratory (as

Table 5. Low to High Gas-Liquid Interaction Flow Regime Transition Data: Air-Water System

Packing Description	D_p, mm	Gas-Liquid System	ρ_L μ_L (*) σ_L	D_c/D_p	Bed Prop. $E_1/E_2/\epsilon$	Source	No. of Points
Glass spheres	3	Air-Water	1 1 72	26.5	215/1.4/0.375	This Work	3
1/16 in. (1.6 mm) Nalco HDS extrudate (**)	1.88	Air-Water	1 1 72	13.5	100/0.8/0.335	This Work	3
Glass spheres	2.9	Air-Water	1 1 72	21.9	180/1.8/0.39	Chou et al.† (1977)	5
Glass spheres	6	Air-Water	1 1 72	13.3	850/2/0.4	Specchia & Baldi (1977)	6
Glass cylinders	2.7	Air-Water	1 1 72	29.6	300/2/0.38	Specchia & Baldi (1977)	5
Glass cylinders	5.4	Air-Water	1 1 72	14.8	500/2.4/0.37	Specchia & Baldi (1977)	6
Porous spheres	3	Air-Water	1 1 72	16.7	207/1.8/0.39	Midoux et al. (1977)	7
Porous cylinders	2.3	Air-Water	1 1 72	21.4	143/3.1/0.39	Midoux et al. (1977)	4
Glass spheres	1.9	Air-Water	1 1 72	26.8	150/1.8/0.344	Tosun (1984)	5

* All systems are at room temperature (22°C) and low pressure (<2 atm).
Air: ρ_{air} = ideal gas value 1.2 to 2.4 kg/m^3; $\mu_{air} = 0.018$ cp.
Units on liquid properties, ρ_L in g/cm^3, μ_L in centipoise, σ_L in dyne/cm.
** From Nalco catalyst company, Chicago, IL; 1/16 in. (1.6 mm) dia. ; $L/D = 2$.
† Chou et al. (1977) did not report the single-phase Ergun equation coefficients for his bed. In this work, the average values reported by MacDonald et al. (1979) were used as representative of this bed.

Table 6. Low to High Gas-Liquid Interaction Flow Regime Transition Data: Nonfoaming Mixtures of Alcohols and Water

Packing Description	D_p, mm	Gas-Liquid System	ρ_L μ_L (*) σ_L	D_c/D_p	Bed Prop. $E_1/E_2/\epsilon$	Source	No. of Points
Glass spheres	2.9	Air-Water-1% Ethanol	0.997 1 66	21.9	180/1.8/0.39	Chou et al. (1977)	6
Glass spheres	2.9	Air-Water-94% Ethanol	0.81 1.1 25	21.9	180/1.8/0.39	Chou et al. (1977)	5
Glass cylinders	5.4	Air-Water-9% Glycerol	1.03 1.26 52	14.8	500/2.4/0.37	Specchia & Baldi (1977)	2
Glass cylinders	5.4	Air-Water-29% Glycerol	1.07 2.34 44	14.8	500/2.4/0.37	Specchia & Baldi (1977)	1
Glass spheres	1.9	Air-Water-80% Methanol	0.8 1 26	26.8	150/1.8/0.344	Tosun (1984)	7
Glass spheres	1.9	Air-Water 28% Glycerine	1.07 2 70	26.8	150/1.8/0.344	Tosun (1984)	8
Glass spheres	1.9	He-Water 50% Glycerine	1.13 5 68	26.8	150/1.8/0.344	Tosun (1984)	5
Glass spheres	1.9	He-Water 80% Methanol	0.8 1 26	26.8	150/1.8/0.344	Tosun (1984)	6
Glass spheres	1.9	He-Water 30% Ethanol 32% Glycerine	1 5 30	26.8	150/1.8/0.344	Tosun (1984)	7

* All systems are at room temperature (22°C) and low pressure (<2 atm).
Air: ρ_{air} = ideal gas value 1.2 to 2.4 kg/m^3; μ_{air} = 0.018 cp.
He: ρ_{Helium} = ideal gas value 0.17 to 0.33 kg/m^3; μ_{He} = 0.02 cp.
Units on liquid properties, ρ_L in g/cm^3, μ_L in centipoise, σ_L in dyne/cm.

explained earlier), literature data (Midoux et al., 1976; Chou et al., 1977; Specchia and Baldi, 1977; Tosun, 1984), and data from private communications (D. H. Anderson, Mobil Oil Company, 1988). The phase and bed properties, as well as the source and number of data points from each source (a total of 157), are given in Tables 5 to 8. The bed and physical property ranges are the same as given for the pressure drop and liquid holdup database with the exception of the minimum surface tension used which was 0.019 N/m. In these tables the data for the low to high interaction regime transition are divided into groups which describe the liquid phase used in the studies (water, nonfoaming aqueous solutions, nonfoaming organic solution, foaming solutions).

The low to high interaction flow regime transition data obtained in our laboratory was taken in conjunction with the hydrodynamic measurements of the low interaction regime. The experimental procedure outlined earlier requires that the high interaction, or pulsing flow regime, be established in each bed prior to pressure drop and holdup measurements in the low interaction regime to ensure uniform distribution of the phases. In each experiment, the high interaction regime, as detected by pressure fluctuations and visual observations, was established in the bed at a particular gas flow rate. The liquid flow rate was then decreased at a constant gas flow rate to establish the low interaction regime with uniform phase distribution. The transition point at a particular gas flow rate was taken to be that liquid flow rate at which all evidence (pressure fluctuations and visual inspection) of the high interaction regime disappeared. This procedure was recommended by Levec et al. (1986) and Tosun (1984) for obtaining uniform phase distribution when transition data can be reproduced by incrementally increasing and decreasing the liquid flow rate. The other transition data which appear in Tables 5 to 8 were obtained under similar procedures by the different authors.

Failure to follow the above procedure and increasing the liquid flow rate from zero at a constant gas flow rate leads to pressure drop hysteresis and nonuniform phase distribution. When phase maldistribution is present at a given gas flow rate, the transition to the high interaction regime occurs at larger liquid flow rates than in cases of uniform distribution (Levec et al., 1986; Christensen et al., 1986; Lazzaroni et al., 1989). Once the high interaction regime is established, decreasing the liquid flow to the low interaction regime leads to a different, lower transition point and uniform phase distribution (that is, the one used in this study). The transition point observed when phase maldistribution is present will not be reproduced during a run once uniform distribution is established in the bed by operation in the high interaction regime. The models of nonuniform phase distribution are insufficient to describe this complicated phenomenon. This work is concerned only with the case of flow regime transitions for uniform phase distribution.

A total database of 157 transition points for a variety of

Table 7. Low to High Gas-Liquid Interaction Flow Regime Transition Data: Nonfoaming Organic Liquids

Packing Description	D_p, mm	Gas-Liquid System	ρ_L μ_L (*) σ_L	D_c/D_p	Bed Prop. $E_1/E_2/\epsilon$	Source	No. of Points
Porous cylinders	1.84	CO_2–Gasoline	0.84 0.57 25	27.2	147/2/0.37	Midoux et al. (1976)	5
Porous cylinders	1.84	N_2–Petroleum Ether	0.65 0.31 19	27.2	147/2/0.37	Midoux et al. (1976)	3
Glass spheres	3	Air–Soybean Oil	0.92 57 29	26.5	215/1.4/0.375	This Work	3
1/16th in. Nalco HDS extrudate**	1.88	Air–Soybean Oil	0.92 57 29	13.5	100/0.8/0.335	This Work	5
Porous Al_2O_3 spheres	3.175	Air–Soybean Oil	0.92 57 29	45	270/2.7/0.46	This Work	3

* All systems are at room temperature (22°C) and low pressure (<2 atm).
Air: ρ_{air} = ideal gas value 1.2 to 2.4 kg/m^3; $\mu_{air} = 0.018$ cp.
CO_2: ρ_{CO_2} = ideal gas value 1.82 to 3.64 kg/m^3; $\mu_{CO_2} = 0.015$ cp.
N_2: ρ_{N_2} = ideal gas value 1.2 to 2.4 kg/m^3; $\mu_{N_2} = 0.018$ cp.
Units on liquid properties, ρ_L in g/cm^3, μ_L in centipoise, σ_L in dyne/cm.
** From Nalco catalyst company, Chicago, IL; 1/16 in. (1.6 mm) dia., $L/D = 2$.

beds and fluids was amassed from the literature, other investigators, and data taken in our laboratory. For approximately 80% of the transition data, inequalities in Eqs. 20b and 20c are satisfied, and the lefthand side of Eq. 20a was found to have an average value of:

$$\text{Average}\left\{\frac{Re_{L,\text{critical}}\Psi_L^{1/11}E_1^{5/11}}{25K^{1/11}}\right\} = 1.22 \pm 0.72$$

This indicates that laminar film instability is a plausible mech-

Table 8. Low to High Gas-Liquid Interaction Flow Regime Transition Data: Foaming Liquids

Packing Description	D_p, mm	Gas-Liquid System	ρ_L μ_L (*) σ_L	D_c/D_p	Bed Prop. $E_1/E_2/\epsilon$	Source	No. of Points
Porous cylinders	1.84	Air–Kerosene I	0.79 0.99 25	27.2	147/2/0.37	Midoux et al. (1976)	4
Porous cylinders	1.84	CO_2–Gas Oil Desulfurized	0.86 5 28.8	27.2	147/2/0.37	Midoux et al. (1976)	5
Porous cylinders	1.84	CO_2-Gas Oil Nondesulfurized	0.86 5 28.3	27.2	147/2/0.37	Midoux et al. (1976)	3
Glass spheres	2.9	Air–Water–50% Ethanol	0.91 1.43 27.5	21.9	180/1.8/0.39	Chou et al. (1977)	5
Glass spheres	2.9	Air–Water–20 ppm Heptyl alcohol	1 1 70	21.9	180/1.8/0.39	Chou et al. (1977)	5
Glass spheres	2.9	Air–Water–1 ppm Surfactant	1 1 61.5	21.9	180/1.8/0.39	Chou et al. (1977)	7
Glass spheres	2.9	Air–Water–2.5 ppm Surfactant	1 1 56.6	21.9	180/1.8/0.39	Chou et al. (1977)	10
Porous Al_2O_3 spheres	3.175	Air–Water–10% Isopropanol	0.96 1.1 41	12.0	140/0.8/0.35	D. H. Anderson Mobil Oil Co.	5

* All systems are at room temperature (22°C) and low pressure (<2 atm).
Air: ρ_{air} = ideal gas value 1.2 to 2.4 kg/m^3; $\mu_{air} = 0.018$ cp.
CO_2: ρ_{CO_2} = ideal gas value 1.82 to 3.64 kg/m^3; $\mu_{CO_2} = 0.015$ cp.
Units on liquid properties, ρ_L in g/cm^3, μ_L in centipoise, σ_L in dyne/cm.

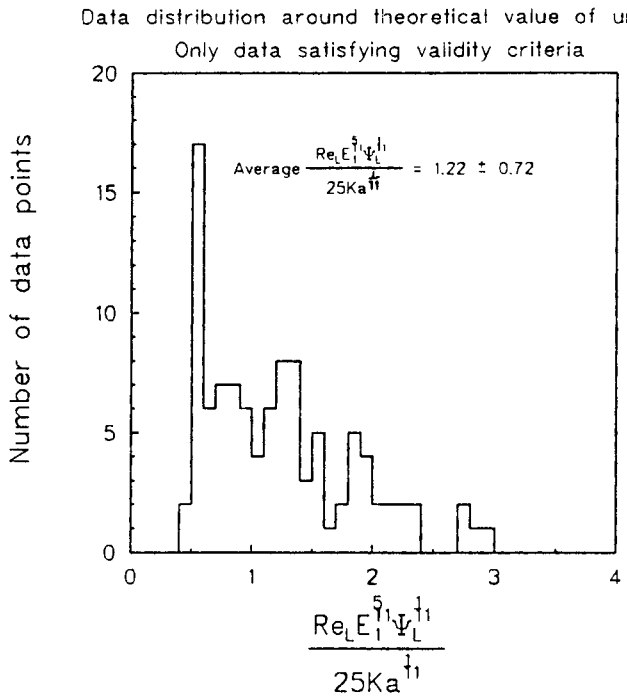

Figure 9. Frequency distribution of the flow regime transition data in Tables 5 to 8 around the theoretical transition value of unity based on laminar film stability.

Only the data which satisfy the validity criteria (Eqs. 20b & c) are shown.

anism of the trickle to pulsing flow regime transition since the theoretically predicted mean is within two standard deviations of the experimental mean. The frequency distribution of the data is shown in Figure 9. If one assumes that $\Psi_L^{1/11}$ is unity (usually close) and the bed and phase properties are known exactly, then the uncertainty in the predicted critical liquid superficial velocity is ±59% when using this average value of the lefthand side of Eq. 20a.

For the data which did not satisfy inequalities in Eqs. 20b and 20c, approximately 18% violated Eq. 20b and 2% violated Eq. 20c. For all the data, the disagreement between the theory and data did show a trend with both the liquid Galileo number and the calculated dimensionless liquid phase pressure drop of the bed so that an empirical correlation was possible. The result is given in the inequality in Eq. 21.

$$\frac{2.9\,Re_{L,\text{critical}}E_1^{5/11}}{\Psi_L^{0.17}Ga_L^{0.41}Ka^{1/11}} \le 1 \tag{21a}$$

$$2.8 < Ga_L < 6.3\times 10^5 \tag{21b}$$

$$1 < \Psi_L < 55 \tag{21c}$$

$$1.2 < L < 12 \text{ kg/m}^2\text{/s} \tag{21d}$$

$$0.004 < G < 2.2 \text{ kg/m}^2\text{/s} \tag{21e}$$

Evaluation of expression in Eq. 21a for all the data (reflected by inequalities in Eqs. 21b to 21e resulted in an average value of:

$$\text{Average}\left\{\frac{2.9\,Re_{L,\text{critical}}E_1^{5/11}}{\Psi_L^{0.17}Ga_L^{0.41}Ka^{1/11}}\right\} = 0.99 \pm 0.30$$

which reflects an improvement in predicting flow regime transition, however, the empirical constants in inequality Eq. 21a are derived from low pressure flow regime transition data only.

Figure 10 compares the predicted and experimental critical liquid flowrates (each at the experimental gas flow rate) for the data appearing in Tables 5 to 8. Figure 10a represents the inequality in Eq. 20a and shows only the data satisfying Eqs. 20b and 20c. Figure 10b is for the empirical correlation, the inequality in Eq. 21a, and shows all the data. For both models most of the data fall within the ±50% confidence limits (75% do in Figure 10a and 90% do in Figure 10b).

Results and Discussion

A model of uniform phase distribution in the trickle flow regime has been developed and is given by Eqs. 16 to 18. The parameters f_v and f_s which were introduced in the development to determine the unknown degree of phase interaction were found to be zero. This results in a final model which has no empirical parameters fitted to two-phase flow data but requires the two Ergun constants determined from single-phase flow experiments on the packing of interest. The absence of adjustable empirical parameters makes this model a good candidate for extension to phase distribution modeling.

In Table 9, we compare this model to other modifications of the Ergun equation. The two-phase flow models of Saez and Carbonell (1985) and Specchia and Baldi (1977) are empirically modified forms of the Ergun equation for single-phase flow and contain parameters fitted to two-phase flow data. The model presented in this work (and by Sweeney (1967)) gives improved prediction of pressure drop and liquid holdup with no empirical parameters determined from two-phase flow data. The models are Larkins et al. (1961), Turpin and Huntington (1967), Midoux et al. (1967), and Ellman et al. (1988). All contain at least four empirical parameters determined from two-phase flow data. The large errors reported for these models in Table 9 are for data in the low interaction regime. No conclusion can be made from our data on the usefulness of the empirical models in the high interaction flow regimes.

All of the data used to develop the hydrodynamic model represent low bed pressures (1 to 2 atmospheres) relative to industrial trickle beds (several hundred atmospheres). The phase interaction parameters, f_v and f_s, determined to be zero from the data on low-pressure beds have not been confirmed to be zero at high gas pressures. After this work was completed, Wammes and Westerterp (1990, 1991) published pressure drop, liquid holdup, and flow regime transition data at pressures up to 60 atmospheres. They used a bed packed with 3 mm glass spheres ($\epsilon = 0.39$), water as the liquid phase, and helium or nitrogen as the gas phase. Unfortunately, the single-phase flow Ergun equation coefficients were not reported for the bed so reliable comparison of the model predictions and data is not possible. However, the universal Ergun equation coefficients recommended by MacDonald et al. (1979), $E_1 = 180$ and $E_2 = 1.8$, gave mean relative errors between the data and pre-

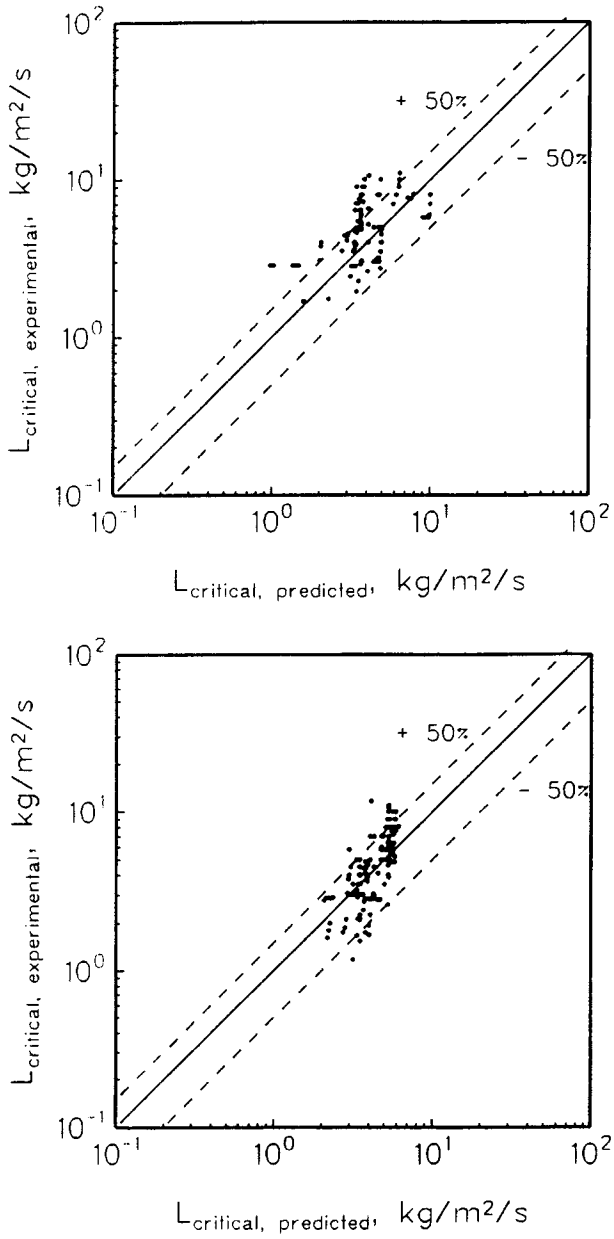

Figure 10. Comparison of the predicted values of critical liquid flow rate to experimental data at the low to high interaction regime transition.

(a) Theory based on laminar film stability, inequality (Eq. 20a), only data which satisfy conditions (Eq. 20b and Eq. 20c) presented as a scatter plot.
(b) Empirical correction to theory, inequality (Eq. 21a).
All low to high interaction flow regime transition data from Tables 5 to 8 presented as a scatter plot.

dictions of $\hat{e}_{\Psi_G} = 67.8\%$ and $\hat{e}_{\epsilon_L} = 16.2\%$. This mean relative error in dimensionless gas pressure drop for the high-pressure system is comparable to the value of 65% which is found when the current model is compared to low-pressure data using the same average values of the Ergun equation coefficients. The mean relative error in the holdup prediction is larger for the high-pressure systems, 16.7% compared to 9.3% for low-pressure system with the universal Ergun coefficients.

The laminar film stability criterion of Kapitza (1945) has been used to predict the trickle to pulsing flow regime transition. Comparison of the model to data indicates that this transition mechanism is statistically significant for the data which satisfy the associated validity conditions (80%). Approximately 20% of the data seem to follow at least two other undetermined mechanisms of flow regime transition. Preliminary conjecture would be that some (18%) follow some type of thick film, pore blockage mechanism, while others (2%) follow a turbulent wave mechanism. At present, an empirical correlation was used to modify the laminar film stability criterion to represent all the atmospheric pressure data (see inequality in Eq. 21).

Table 9. Comparison of Published Model Predictions of Pressure Drop and Liquid Holdup to the Database

Model	$\hat{e}_{\Psi_G}$	$\hat{e}_{\epsilon_L}$
This work, Eqs. 20 to 22 Sweeney (1967)	44%	11%
Sáez and Carbonell (1985) Universal Ergun coefficients Measured static holdup*	106%	15.7%
Specchia and Baldi (1977) Ergun coefficients for wet packing Measured static holdup*	143%	17.9%
Larkins et al. (1961)**	297%	48.3%
Turpin and Huntington (1967)	256%	30.3%
Midoux et al. (1976)**	190%	36.5%
Ellman et al. (1988)	62.7%	43.2%

* The use of measured static holdup was found to give lower errors than the use of the correlation proposed by Sáez and Carbonell (1985).
** The measured values of the Ergun equation constant for single-phase flow were used for these correlations.

Figure 11a compares the predicted and experimental critical liquid flow rates (each at the experimental gas flow rate) at the trickle to pulsing flow regime transition for the model of Ng (1986). The hydrodynamic model given in Eqs. 16 to 18 was used to calculate the liquid holdup required by this model. Most of the data (70%) are within the ±50% confidence limits; however, the data which are outside these limits are predicted poorly. Figure 11b shows only the data which violate inequality in Eq. 20b and which have been conjectured to represent a thick film pore blockage mechanism. Ng's (1986) model is based on pore blockage. As can be seen, the data which deviate the most from Ng's (1986) model are also those which violate inequality in Eq. 20b. This result gives no additional insight into the transition mechanism of these data.

Figure 12 compares the predicted and experimental critical liquid flow rates (each at the experimental gas flow rate) at the trickle to pulsing flow regime transition for the model of Grosser et al. (1988). The hydrodynamic model given in Eqs. 16 to 18 was used as a basis for their models rather than the empirical model of Saez and Carbonell (1985). Their model based on gas compressibility and the existence of a solution to the one-dimensional volume averaged momentum balance (Figure 12b) overpredicts the critical liquid flow rates to such an extent that none of the predictions are within the ±50% confidence limits. Their model based on a stability analysis of the one-dimensional volume averaged momentum balance

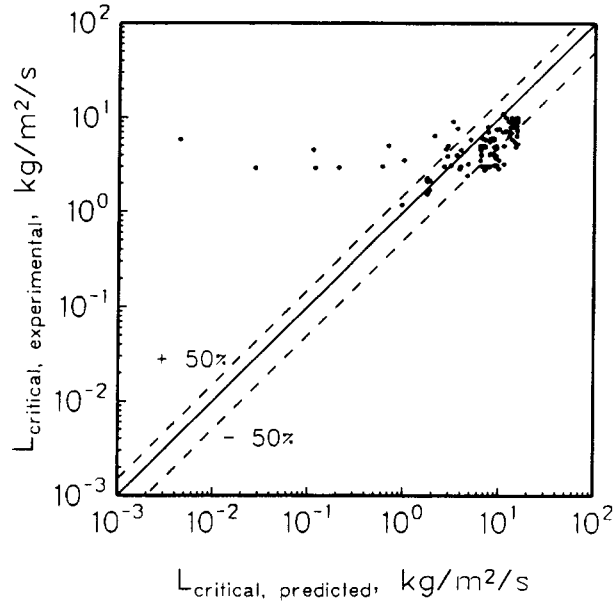

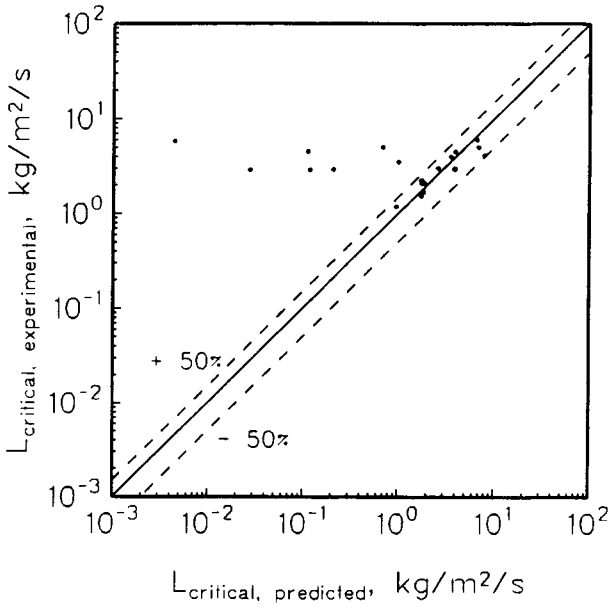

Figure 11. Comparison of the predicted values of critical liquid flow rate to experimental data at the low to high interaction regime transition.

(a) Ng (1986). Only the low to high interaction flow regime transition data from Tables 5 to 8 which had positive predicted $L_{critical}$ presented as a scatter plot.
(b) Ng (1986). Only data which does not satisfy inequality (Eq. 20b) and is suspected of having a transition mechanism based on pore blockage.

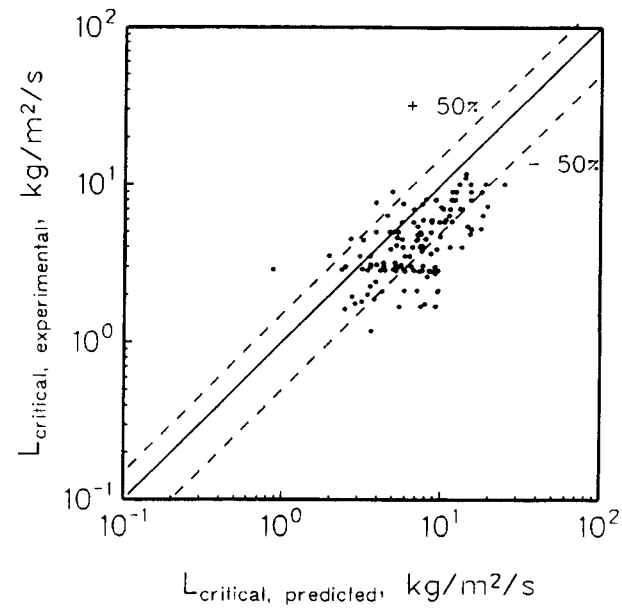

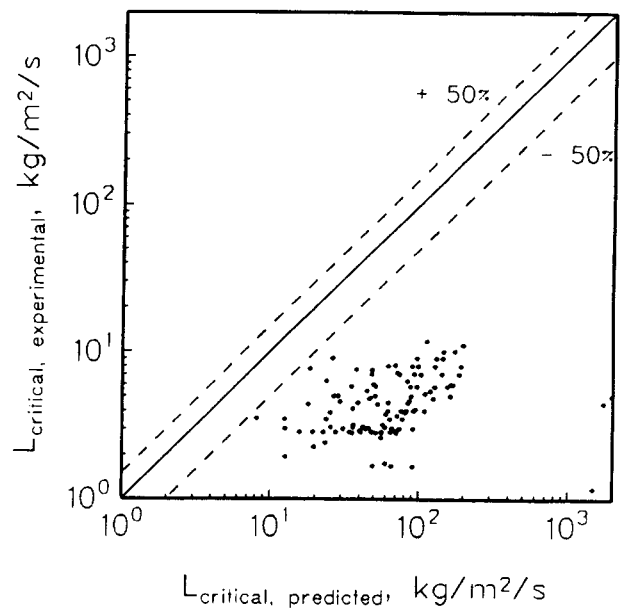

Figure 12. Comparison of the predicted values of critical liquid flow rate to experimental data at the low to high interaction regime transition.

(a) Grosser et al. (1988) Model I (based on stability analysis).
(b) Grosser et al. (1988) Model II (based on existence of solution to one-dimension volume averaged momentum balance).
All low to high interaction flow regime transition data from Tables 5 to 8 presented as a scatter plot.

ure 12a) does very well with 77% of the predictions falling within the ±50% confidence limits.

Figure 13 compares the laminar film stability criterion with two data sets of Tosun (1984) from Table 6. Tosun's (1984) data for the trickle to dispersed bubble and pulsing to dispersed bubble transition are shown for completion. The transition models of Ng (1986) and Grosser et al. (1988) are also shown for reference. The laminar film stability criterion seems to predict the trickle to pulsing flow regime transition more consistently than the other models in these and most other data sets. However, it is obvious that the other flow regime boundaries, specifically the trickle to dispersed bubble transition, are not predicted by the model based on laminar film stability. We can conclude that the mechanism of these other transitions is not laminar film instability, even though correct mechanisms are not known at this time.

All of the data used to develop the flow regime transition models also represent low bed pressures (1 to 2 atm) relative to industrial trickle beds (several hundred atmospheres). As

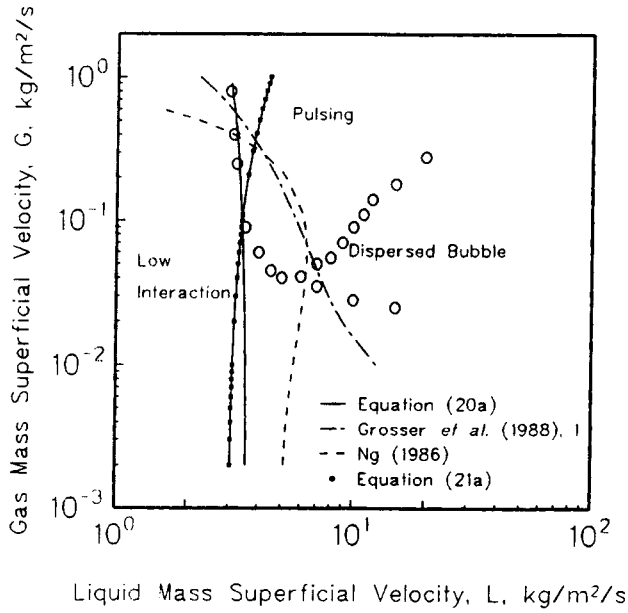

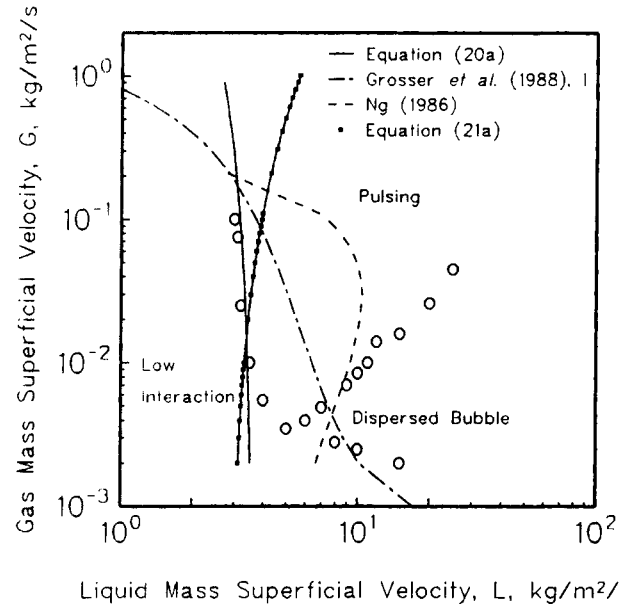

Figure 13. Operating diagram for 80% methanol in water with (a) air and (b) helium.

Data of Tosun (1984). Model predictions of laminar film stability model (Eq. 20a), Ng (1986), and Grosser et al. (1988), Model II.

previously mentioned, Wammes and Westerterp (1990, 1991) have published some flow regime transition data in trickle beds with pressures as high as 60 atmospheres. In Figure 14, the various model predictions of critical liquid flow rate with increasing gas pressure (or density) are compared with some of this data. As can be seen, only the empirical correlation, Eq. 21, predicts the correct trend with increasing gas pressure. This result indicates that the mechanisms of flow regime transition which have been developed with some success for low-pressure systems do not apply at high gas pressures. The empirical correlation shows some promise, but a more extensive database of high-pressure hydrodynamics is needed to fully understand its effectiveness.

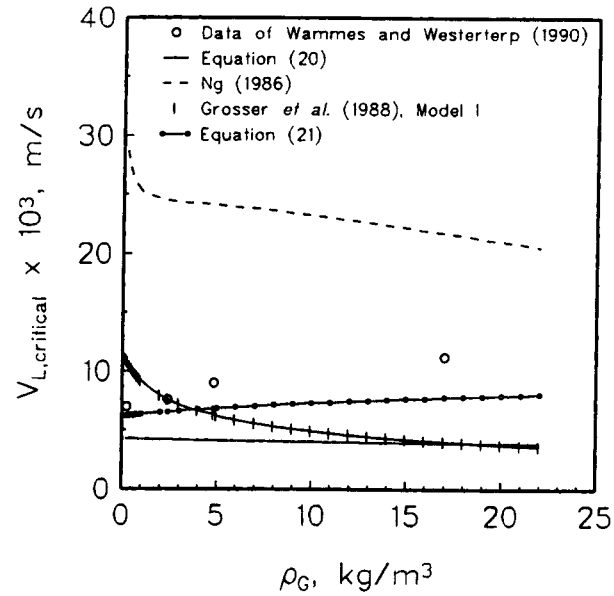

Figure 14. Comparison of trickle to pulsing flow regime transition data at high gas pressures (Wammes and Westerterp, 1990) to several model predictions.

Liquid phase is water. Bed properties are $D_p = 3$ mm, $\epsilon = 0.39$, $E_1 = 180$, $E_2 = 1.8$. Gas viscosity set at 0.018 cp.

Summary and Conclusions

A model of cocurrent gas-liquid film flow in a slit geometry can be used with proper geometrical mapping to describe trickle flow in packed beds. When such a model is based on the universal velocity profile in each phase, comparison of the model predictions for pressure drop and liquid holdup with data indicate an absence of interaction at the gas-liquid interface (that is, slip in velocity and shear discontinuity). This can be rationalized since the steady-state phenomenological model is attempting to capture much more complex periodic or chaotic phenomena on the pore scale. The final form of this phenomenological model assumes the form proposed, based on heuristic arguments, by Sweeney (1967). The model requires Ergun constants to be determined for each packing of interest by single-phase flow experiments on dry packing, but contains no empirical constants fitted to two-phase flow data. This makes the model particularly desirable for use with new packing shapes. Model predictions for pressure drop and liquid holdup, confined to the trickle flow regime, are superior to those of other models. Pressure drop and liquid holdup are predicted with 42% and 10.7% mean relative error, respectively. While this is an improvement over other available correlations and models, these high levels of error indicate that uniform phase distribution in trickle flow is very difficult to achieve and maintain. Improved predictions might require a more accurate description of the bed void geometry.

A liquid holdup model was also derived for liquid film flow under stagnant gas conditions as a limiting case of the above model. It contains no adjustable parameters. This model also requires the Ergun constants from single-phase gas flow experiments to characterize the different packings. For the air-water systems, a mean relative error of 6.3% was found between the model predictions and the liquid holdup data. For

the air-soybean oil systems, the mean relative error is 11.2%. This increase in error reflects the regions of poor liquid distribution in our apparatus when using a high viscosity liquid in the absence of gas flow. The success of the stagnant gas model for lower viscosity liquids supports the view that liquid flow can be modeled as thin films over the packing surface for the particle sizes used in trickle beds when liquid distribution is uniform. The question of (lack of) uniformity can only be addressed by some imaging technique and computer tomography.

Mapping Kapitza's (1945) criterion for laminar film instability to bed variables leads to the prediction of trickle to pulse flow regime transitions which are comparable or better than those of other models. The so developed transition criterion contains no empirical parameters and predicts transition data in trickle beds that satisfy the constraints imposed by the development (80% of the transition data satisfied the constraints). Of the data satisfying the constraints, 75% of all the predicted critical liquid flow rates (at specified gas flow rates) were within ±50 percent of the experimental values. This transition mechanism was also shown to be statistically significant since the normalized theoretical predictions lie within two standard deviations of the experimental average.

The models by Ng (1986) (pore scale model) and Grosser et al. (1988) (bed scale model) also compared well to the same trickle to pulsing flow regime transition data. Each of these models require the hydrodynamic parameters of pressure drop and liquid holdup for two-phase flow in the low interaction regime. The hydrodynamic model developed in this work was used in all cases to give a common basis for comparison. The model developed by Ng (1986), based on a clogged pore transition mechanism, was found to predict the critical liquid flow rates such that 70% were within the ±50% confidence limits. However, the data outside these confidence limits were very poorly predicted, even for small particles and viscous fluids when his assumed transition mechanism seems physically realistic. Grosser's et al. (1988) model based on gas compressibility was found to always predict higher values of the critical liquid flow rate (for a particular gas flow rate) than are measured experimentally (no data within ±50%). Grosser's et al. (1988) model based on a stability analysis of the one-dimensional volume averaged steady-state momentum balance was found to predict the critical liquid flow rate such that 77% of data were within the ±50% confidence limits. For an *a priori* prediction of the trickle to pulsing flow regime transition, only the model developed in this work based on laminar film instability and Grosser et al.'s (1988) model based on a stability analysis have been shown to give reliable results in low-pressure systems. For the limited amount of data available on high-pressure systems, only the empirical correlation, Eq. 21, predicted the correct trend of critical liquid flow rate with increasing gas density.

The results of this study indicate that a pore scale phenomenological model can be at least as successful in predicting bed scale phenomenon as empirical correlations or bed scale models. This situation can only change if more accurate descriptions of void scale phase interaction terms become available for incorporation in volume averaged bed scale models.

Acknowledgments

These investigations were entirely funded by the industrial sponsors of the Chemical Reaction Engineering Laboratory of Washington University to whom we are indebted. Additionally, R. A. Holub would like to extend his gratitude to the Amoco Oil Company which sponsored the fellowship he received for three years of his graduate work.

Notation

D_p = equivalent spherical diameter of the packing particle
$\hat{e}_\phi$ = mean relative error between a measured and predicted value of the function ϕ, see Eq. 15
E_1 & E_2 = constants of the Ergun equation for single-phase flow on the packing of interest (describe bed tortuosity and roughness)
g = gravitational acceleration
Ga_α = bed Galileo number of the α phase, $(g D_p^3 \epsilon^3)/[\nu_\alpha^2(1-\epsilon)^3]$
G = gas mass superficial velocity = $\rho_G V_G$
Ka = Kapitza number of the liquid phase = $(\sigma_L/\rho_L)^3/g\nu_L^4$
L = liquid mass superficial velocity = $\rho_L V_L$
L_{bed} = bed length over which pressure drop is measured
P = absolute pressure
Re_α = bed Reynolds number of the α phase, $(V_\alpha D_p)/[\nu_\alpha(1-\epsilon)]$
Re'_α = slit Reynolds number of the α phase, $(\langle v_\alpha \rangle w)/\nu_\alpha$
S_D = half wall thickness of the average slit in the system of slits model
v_α = velocity of the subscripted phase in the slit, the interstitial phase velocity
V_α = superficial velocity of the α phase
w = half width of the average slit in the system of slits model

Greek letters

δ = liquid film thickness in the average slit in the system of slits model
ϵ = bed porosity
ϵ_α = bed holdup of the α phase
η_α = pseudo-bed Reynolds number based on shear stress in the α phase and the phase holdup = $(1/5E_1^{0.25})\sqrt{E_1 Re_\alpha + E_2 Re_\alpha^2}$
θ = angle of inclination from vertical for the average slit in the system of slits model
μ_α = viscosity of the α phase
ν_α = kinematic viscosity of α phase, μ_α/ρ_α
ρ_α = density of the α phase
σ_l = surface tension coefficient of the liquid relative to the gas
τ_α = characteristic shear in the α phase
Ψ_α = dimensionless body force on the α phase = $1/\rho_\alpha g\,[-\Delta P/L_{bed} + \rho_\alpha g]$

Subscripts

α = general subscript meaning gas (G) or liquid (L)
critical = quantity specified at a flow regime transition point
bed = quantity defined for the bed
ϕ = general subscript meaning some function, such as pressure drop or holdup
G = gas phase
i = gas liquid interface
L = liquid phase
slit = quantity defined for the average slit in the system of slits model

Superscripts

o = static or residual liquid holdup after drainage

Miscellaneous

$\langle\ \rangle$ = intrinsic phase average of the enclosed variable in the slit
$<\ >$ = arithmetic average of the enclosed variable

Literature Cited

Anderson, D. H., Mobil Oil Corporation, private communication (1985).

Baker, O., "Simultaneous Flow of Oil and Gas," *Oil and Gas J*, 185 (July 26, 1954).

Blok, J. R., J. Varkevisser, and A. A. H. Drinkenberg, "Transition to Pulsing Flow, Holdup, and Pressure Drop in Packed Columns with Cocurrent Gas-Liquid Downflow," *Chem. Eng. Sci.*, **38**, 687 (1983).

Charpentier, J. C., C. Prost, and P. LeGoff, "Chute de Pression pour des Écoulements à Garnissage Arrosé: Comparaison avec le Garnissage Noyé," *Chem. Eng. Sci.*, **24**, 1777 (1969).

Chou, T. S., F. L. Worley, Jr., and D. Luss, "Transition to Pulsed Flow in Mixed-Phase Cocurrent Downflow through a Fixed Bed," *Ind. and Eng. Chem., Proc. Design and Dev.*, **16**, 424 (1977).

Christensen, G., S. J. McGovern, and S. Sundaresan, "Cocurrent Downflow of Air and Water in a Two Dimensional Packed Column," *AIChE J.*, **32**, 1677 (1986).

Clements, L. D., and P. C. Schmidt, "Two-Phase Pressure Drop in Cocurrent Downflow in Packed Beds: Air-Silicone Oil Systems," *AIChE J.*, **26**, 314 (1980).

Dudukovič, M. P., and P. L. Mills, *Encyclopedia of Fluid Mechanics*, Chapter 32, Gulf Publishing Company, Houston, TX (1986).

Dukler, A. E., and O. P. Bergelin, "Characteristics of Flow in Falling Liquid Films," *Chem. Eng. Prog.*, **48**, 557 (1952).

Ellman, M. J., N. Midoux, A. Laurent, and J. C. Charpentier, "A New, Improved Pressure Drop Correlation for Trickle Bed Reactors," *Chem. Eng. Sci.*, **43**, 2201 (1988).

Ergun, S., "Fluid Flow through Packed Columns," *Chem. Eng. Prog.*, **48**, 89 (1952).

Fukushima, S., and K. Kusaka, "Interfacial Area and Boundary of Hydrodynamic Flow Region in Packed Column with Cocurrent Downward Flow," *J. of Chem. Eng. Japan*, **10**, 461 (1977a).

Fukushima, S., and K. Kusaka, "Liquid Phase Volumetric and Mass Transfer Coefficient, and Boundary of Hydrodynamic Flow Region in Packed Column with Cocurrent Downward Flow," *J. of Chem. Eng. Japan*, **10**, 468 (1977b).

Fukushima, S., and K. Kusaka, "Boundary of Hydrodynamic Flow Region and Gas Phase Mass Transfer Coefficient in Packed Column with Cocurrent Downward Flow," *J. of Chem. Eng. Japan*, **11**, 241 (1978).

Grosser, K., R. G. Carbonell, and S. Sundaresan, "Onset of Pulsing in Two-Phase Cocurrent Downflow through Packed Beds," *AIChE J.*, **34**, 1850 (1988).

Hanratty, T. J., and J. M. Ergen, "Interaction Between a Turbulent Air Stream and a Moving Liquid Surface," *AIChE J.*, **3**, 299 (1957).

Holub, R. A., "Hydrodynamic of Trickle Bed Reactors," D.Sc. Thesis, Washington University, St. Louis, MO (1990).

Holub, R. A., M. P. Dudukovič, and P. A. Ramachandran, "Hydrodynamics of Trickle Bed Reactors: A Diagnostic Model of Phase Maldistribution," AIChE Annual Meeting, Washington, DC, paper 45a (November 1988).

Kan, K., and P. F. Greenfield, "Multiple Hydrodynamic States in Cocurrent, Two-Phase Downflow through Packed Beds," *Ind. and Eng. Chem., Process Design and Development*, **17**, 482 (1975).

Kapitza, P. L., "Wave Flow of Thin Layers of a Viscous Fluid," *Collected Works of P. L. Kaptiza*, D. ter Haar, ed., Pergamon Press, Oxford (1965).

Larkins, R. P., R. R. White, and D. W. Jeffrey, "Two-Phase Cocurrent Flow in Packed Beds," *AIChE J.*, **7**, 231 (1961).

Lazzaroni, C. L., H. R. Keselman, and N. S. Figoli, "Trickle Bed Reactors. Multiplicity of Hydrodynamic States. Relation Between Pressure Drop and the Liquid Holdup," *Ind. and Eng. Chem. Res.*, **28**, 119 (1989).

Levec, J., A. E. Sáez, and R. G. Carbonell, "The Hydrodynamics of Trickling Flow in Packed Beds, Part II: Experimental Observations," *AIChE J.*, **31**, 369 (1986).

Levec, J., K. Grosser, and R. G. Carbonell, "The Hysteretic Behavior of Pressure Drop and Liquid Holdup in Trickle Bed Reactors," *AIChE J.*, **34**, 1027 (1988).

MacDonald, I. F., M. S. El-Sayed, K. Mow, and F. A. L. Dullien, "Flow through Porous Media—the Ergun Equation Revisited," *Ind. and Eng. Chem. Fund.*, **18**, 199 (1979).

Midoux, N., M. Favier, and J. C. Charpentier, "Flow Pattern, Pressure Loss, and Liquid Holdup Data in Gas-Liquid Downflow Packed Beds with Foaming and Nonfoaming Hydrocarbons," *J. of Chem. Eng. of Japan*, **9**, 305 (1976).

Ng, K. M., "A Model for Flow Regime Transitions in Cocurrent Downflow Trickle Bed Reactors," *AIChE J.*, **32**, 115 (1986).

Pike, J. G., "Influence of a Falling Thin Liquid Film Upon a Co-Currently Flowing Gas Stream in a Vertical Duct," *Canadian J. of Chem. Eng.*, 267 (Oct., 1965).

Ramachandran, P. A., and R. V. Chaudhari, *Three Phase Catalytic Reactors*, Gordon and Breach Science Publishers, NY (1983).

Ramachandran, P. A., M. P. Dudukovič, and P. L. Mills, "Recent Advances in the Analysis and Design of Trickle Bed Reactors," *Sadhana, Proceedings of the Indian Academy of Sciences*, **10**, 269 (1987).

Sáez, A. E., and R. G. Carbonell, "Hydrodynamic Parameters for Gas-Liquid Cocurrent Flow in Packed Beds," *AIChE J.*, **31**, 52 (1985).

Sai, P. S. T., and Y. B. G. Varma, "Flow Pattern of the Phases and Liquid Saturation in Concurrent Downflow through Packed Beds," *The Canadian J. of Chem. Eng.*, **60**, 353 (1988).

Sai, P. S. T., and Y. B. G. Varma, "Pressure Drop in Gas-Liquid Downflow through Packed Beds," *AIChE J.*, **33**, 2027 (1987).

Sato, Y., T. Hirose, F. Takahashi, and M. Toda, "Pressure Loss and Liquid Holdup in Packed Bed Reactor with Cocurrent Gas-Liquid Downflow," *J. of Chem. Eng. Japan*, **6**, 147 (1973a).

Sato, Y., T. Hirose, F. Takahashi, M. Toda, and Y. Hashiguchi, "Flow Pattern of Cocurrent Gas-Liquid Downflow in Packed Bed Reactor," *J. of Chem. Eng. Japan*, **6**, 315 (1973b).

Scheideggar, A. E., *The Physics of Flow through Porous Media*, MacMillan, NY (1957).

Sicardi, S., H. Gerhard, and H. Hoffman, "Flow Regime Transition in Trickle Bed Reactors," *The Chem. Eng. J*, **18**, 173 (1979).

Sicardi, S., and H. Hoffman, "Influence of Gas Velocity and Packing Geometry on Pulsing Inception in Trickle Bed Reactors," *The Chem. Eng J.*, **20**, 251 (1980).

Specchia, V., and G. Baldi, "Pressure Drop and Liquid Holdup for Two Phase Concurrent Flow in Packed Beds," *Chem. Eng. Sci.*, **32**, 515 (1977).

Sweeney, D. E., "A Correlation for Pressure Drop in Two Phase Concurrent Flow in Packed Beds," *AIChE J.*, **13**, 663 (1967).

Talmor, E., "Two Phase Downflow through Catalyst Beds: Part 1. Flow Maps," *AIChE J.*, , **23**, 868 (1977).

Tosun, G., "A Study of Cocurrent Downflow of Nonfoaming Gas-Liquid Systems in Packed Bed: 1. Flow Regime: Search for a Generalized Flow Map, 2. Pressure Drop: Search for a Correlation," *Ind. and Eng. Chem., Proc. Design and Devel.*, **23**, 29 (1984).

Turpin, J. L., and R. L. Huntington, "Prediction of Pressure Drop for Two-Phase, Two-Component Concurrent Flow in Packed Beds," *AIChE J.*, **6**, 1196 (1967).

Wammes, W. J. A., and K. R. Westerterp, "The Influence of the Reactor Pressure on the Hydrodynamics in a Cocurrent Gas-Liquid Trickle Bed Reactor," *Chem. Eng. Sci.*, **45**, 2247 (1990).

Wammes, W. J. A., J. Middelkamp, W. J. Huisman, C. M. deBaas, and K. R. Westerterp, "Hydrodynamics in a Cocurrent Gas-Liquid Trickle Bed at Elevated Pressures: Part 2 Liquid Holdup, Pressure Drop, Flow Regimes," *AIChE J.*, **37**, 1855 (1991).

Manuscript received Dec. 6, 1991, and revision received Aug. 24, 1992.